mouse peritoneal macrophages is mediated by SR-AI/II and that CD36 accounts for an additional 35% of oxLDL degradation (12, 13). In peritoneal macrophages from mice lacking both SRAI/II and CD36, degradation of oxLDL was reduced by 75% (13). It has been suggested that LOX-1 may also be an important receptor for oxLDL in macrophages (14), but to date no studies have provided a quantitative estimate of the contribution of LOX-1 to oxLDL uptake by macrophages.

We recently showed that oxidized LDL blocks apoptosis in macrophages through activation of the phosphatidylinositol 3-kinase/protein kinase B (PI3K/PKB) cascade, translocation of NF- B to the nucleus, and induction of the anti-apoptotic factor $BclX_L$ (15, 16). Our preliminary results in SR-AI/II macrophages (17) and CD36 knockout macrophages (unpublished) suggest that the anti-apoptotic effect of oxLDL does not require either of these two scavenger receptors. LOX-1 was deemed an attractive candidate because its much higher affinity for oxidized LDL compared with acetyl LDL or native LDL is congruent with the finding that oxLDL (but not acetyl LDL or native LDL) can inhibit apoptosis in macrophages and because it has been shown to be involved in survival signaling and NF- B activation (4, 6, 18).

In the present study we describe results of experiments using LOX-1 knockout mice to examine the role the LOX-1 receptor plays in mediating uptake of, and signaling by, ox-LDL in macrophages.

MATERIALS AND METHODS

Materials

Carrier-free Na ^{125}I was purchased from Perkin Elmer (Woodbridge, Ontario). DMEM, αMEM medium, propidium iodide, and RNase A were obtained from Invitrogen (Burlington, ON, Canada). Defined fetal bovine serum (FBS) was from HyClone (Logan, UT). Promega (Madison, WI) supplied 3-(4,5-Dimethylthiazol-2-yl)-5-(3-carboxymethoxyphenyl)-2-(4-sulfophenyl)-2*H*-tetrazolium, inner salt (MTS). Phenazine methosulfate (PMS) and 1-stearoyl lysophosphatidylcholine were from Sigma Aldrich (St. Louis, MO). Centriplus 20 ultrafilters were purchased from Amicon (Beverly, MA). Molecular Probes (Eugene OR) provided 1,1′-dioctadecyl-3,3,3′,3′-tetramethylindocarbocyanine perchlorate (DiI). Anti-CD68 was purchased from Serotec (Raleigh, NC). Primary antibody against p85 subunit of PI3K was purchased from Santa Cruz Biotechnology (Santa Cruz, CA). Antibodies against total and phosphorylated PKB (Ser470) were from Cell Signaling Technology (Beverly, MA).

Animals

Inactivation of the single-copy murine LOX-1 receptor gene by homologous recombination was performed in the laboratory of Dr. T. Sawamura (9). Offspring with the inactivated gene in germine cells were backcrossed 8 times onto a C57bl/6 background. LOX-1 genotypes were verified by PCR analysis of tail DNA in all breeding animals, as well as in selected experimental animals. DNA was extracted using a Qiagen DNeasy kit. The forward primer for the LOX-1 deletion was 5′-CAGCGAACACAGCTCCGTCTTGAAGG-3′ and the reverse primer was 5′-GGCCAACCATGGCTTGGGAGAATGG-3′. The forward primer for the neomycin-resistance cassette was 5′-CAACGCTATGTCCTGATAGCGGTCC-3′ and the reverse primer was 5′-CGTGTTCCGGCTGTCAGCGCAGG-3′. Wild-type C57bl/6 mice were purchased from The Jackson Laboratory. All animal procedures were in accordance with the guidelines of the Canadian Council on Animal Care and were approved by the Animal Care Committee of the University of British Columbia.

Lipoprotein isolation and labeling

LDL (d = 1.019–1.063 g/ml) was isolated by sequential ultracentrifugation of EDTA-anticoagulated fasting plasma obtained from healthy normolipidemic volunteers (19). Radioiodination was performed using a modification of the iodine monochloride method of MacFarlane (20). The specific activity was between 100 and 150 cpm/ng LDL protein. Iodination was performed before oxidation or acetylation of LDL. Lipoprotein-deficient serum (LPDS) was prepared from the d > 1.25 fraction.

LDL modification

LDL was oxidized by incubating 200 μg/ml LDL in PBS containing 5 μmol/L $CuSO_4$ at 37°C for 20 h (21). OxLDL was then washed and concentrated to about 1 mg/ml with Centriplus 20 ultrafilters (Millipore, Bedford, MA). Agarose gel electrophoresis typically showed a 4-fold increase in electrophoretic mobility for oxidized LDL compared with native LDL. LDL was acetylated by adding four 1-μl aliquots of acetic anhydride at 10 min intervals to 2 mg of LDL in 600 μl of ice-cold 50% saturated sodium acetate (22).

Macrophage isolation and culture

Peritoneal macrophages were obtained from wild-type or LOX-1 knockout C57/bl mice by peritoneal lavage with ice-cold Ca^{2+}-free Dulbecco's PBS. Macrophages were suspended in α-minimal essential medium (α-MEM) with 10% fetal bovine serum (FBS) and plated in 12-well plastic culture plates. Nonadherent cells were removed by medium exchange after 1 h. Adherent macrophages were cultured overnight, washed with α-MEM, and then used for experiments. Bone marrow cells were isolated from the femurs of 6–8-week-old female C57/bl mice as described previously (22). Cells were plated for 24 h in RPMI 1640 containing 10% FBS and 10% L-cell conditioned medium as the source of M-CSF. The nonadherent cells were removed and cultured in the above medium for 5–7 days until 80% confluence was reached.

Reverse transcription polymerase chain reaction analysis

RNA was isolated from BMDM and peritoneal macrophages (PM) from wild-type or LOX-1 knockout mice using Trizol (Invitrogen, Burlington, ON). Total RNA was then used as a template for first strand cDNA synthesis using M-MLV reverse transcriptase from Promega (Madison, WI) according to the manufacturer's instructions. The resulting cDNA was amplified using the forward primer 5′-CGTGTTCCGGCTGTCAGCGCAGG-3′ and the reverse primer 5′-CAACGCTATGTCCTGATAGCGGTCC-3′. These sequences were obtained from the genomic sequence using the algorithm Primer 3 (www-genome.wi.mit.edu/cgi-bin/primer/primer3_www.cgi). PCR was performed with Taq DNA polymerase (Invitrogen, Burlington, ON) in a 25 μl reaction volume containing 10 pmol of each primer. Amplification was performed for 35 cycles at 94°C for 2 min, 94°C for 40s, 60°C for 1 min, and 72°C for 1 min. The final elongation phase was done at 72°C for 10 min. The PCR products were electrophoresed on a 1.5% agarose gel and visualized using ethidium bromide under UV light.

Fluorescent labeling

Fluorescent labeling of oxLDL was performed by adding 100 μg DiI in 60μl dimethyl sulfoxide to 2 mg of oxLDL in the pres-

ence of d > 1.21g/ml plasma fraction as a source of lipid transfer activity (24). Following an 8 h incubation period at 37°C, the labeled oxLDL was reisolated by ultracentrifugation at d = 1.1. This procedure typically resulted in an incorporation of 5–15 μg of DiI per mg of LDL protein.

Assays of LDL uptake and degradation in cultured cells

Macrophages were incubated at 37°C with varying concentrations of radioiodinated native, oxidized, or acetylated LDL in α-MEM with 2.5% lipoprotein deficient serum. After 4 h, the medium was removed and the cells were washed. LDL degradation products were quantified by mixing 1 ml of the supernatant medium with 350 μl of 50% trichloroacetic acid and 350 μl of 7.5% $AgNO_3$. The mixture was centrifuged at 2500 rpm for 15 min, and the supernatant was counted on a LKB 1282 γ counter. The cells were removed from the plates with Teflon cell lifters and counted to determine cell-associated LDL.

Uptake of DiI labeled oxLDL by macrophages

Peritoneal macrophages were incubated for 5 h at 37°C with 10 μg/ml DiI-labeled oxidized LDL in α-MEM containing 2.5% LPDS. Cells were washed with PBS, fixed with 2% formaldehyde, and mounted in 90% glycerol, 9.75% PBS, and 0.25% 1,4-diazabicyclo[2,2,2]octane. Cells were examined with a Zeiss Axioskop fluorescence microscope in epifluorescent mode with a fluorescein filter set.

In vivo clearance of LDL

Clearance of oxLDL or native LDL was measured as previously described (25). Briefly, wild-type or LOX-1 deficient mice were anesthetized with 2% isoflurane. The external jugular vein was exposed with the aid of a Zeiss operating microscope (Carl Zeiss Canada Ltd., Don Mills, Ontario) and cannulated with a PE 10 polyethylene catheter (outer diameter 0.61 mm; VWR Canlab), positioned with its tip in the superior vena cava. ^{125}I oxLDL (1-2 million cpm) in 200 μl of 150 mM NaCl was drawn into a 1ml syringe. The syringe was counted before and after the injection to allow an accurate determination of the amount of radioactivity administered. Five or six 20 μl blood samples were collected over 20 min. A second injection was then performed with a similar amount of native LDL, and four or five 20 μl samples were collected over 20 min. For oxLDL, the concentration at zero time was calculated using the injected dose of oxLDL and the volume of distribution of native LDL.

Cell viability assay

Macrophage survival was determined by the MTS-formazan method. This assay is based on the cellular bioreduction of MTS by mitochondrial dehydrogenase enzymes in metabolically active cells. The quantity of formazan product formed was measured by the absorbance at 490 nm and is directly proportional to the number of viable cells in culture (26). MTS-PMS solution (20 μl/well) was added to wells containing 100 μl of culture medium in 96 well plates for 3 h before terminating the experiment. This resulted in final MTS and PMS concentrations of 333 μg/ml and 25 μM, respectively. After 3 h incubation at 37°C in a humidified 5% CO_2 atmosphere, the absorbance at 490 nm was recorded with an ELISA plate reader.

Apoptosis assay

Propidium iodide staining and FACS analysis was used to quantitate the subdiploid population. At the end of 24 hr incubation, BMDM from wild-type or LOX-1 knockout mice were fixed and permeabilized with ethanol 70% (v/v) for 1 h at 4°C and washed twice in PBS containing 0.01% glucose. Cells were then resuspended in the same buffer plus RNase A (final concentration 0.1 mg/ml) and propidium iodide (final concentration 0.12 mg/ml). Fluorescence was measured with a BD FACS Canto. The data was analyzed with FCS Express Pro Software Version 3 (De Novo Software, Thornhill, Canada) with gating to exclude debris and cellular aggregates.

Immunoblotting

BMDM were harvested as described above and lysed in ice-cold homogenization buffer [20 mM morpholinepropanesulfonic acid, pH 7.2, 1% Triton X-100, 50 mM β-glycerol phosphate, 5 mM EGTA, 2 mM EDTA, 1 mM sodium vanadate, 25 μM β-methyl aspartic acid, 1 mM DTT, 1 mM phenylmethylsulfonyl fluoride, aprotinin (10 μg/ml), and leupeptin (10 μg/ml)]. Lysates were centrifuged at 14,000 rpm for 10 min, and the protein content of supernatants was quantified using the Bradford protein assay. Fifty micrograms of protein from each sample was loaded and separated by SDS-PAGE using a 10% separating gel. Gels were calibrated with prestained SDS-PAGE low molecular weight standards (Bio-Rad, Hercules, CA). Proteins were then transferred to nitrocellulose membranes which were then blocked for 1 h with 4% skim milk, 0.01% NaN_3 in TBS-0.1% Tween 20. The membranes were cut at about the 70 kDa point, and the bottom section was then incubated with anti-phospho(Ser473) PKB antibody overnight in TBS-0.1% Tween 20 at 4°C, washed three times, and then incubated with horseradish peroxidase-conjugated secondary antibody at a 1:5,000 dilution for 1 h. The bands were then visualized by enhanced chemiluminescence. This blot was then stripped in Tris buffer containing SDS (2%) and β-2-mercaptoethanol (100 mM) at 50°C for 20 min, washed, and reprobed with antibody to PKB. The top section of the membrane was incubated with antibody against the p85 subunit of PI3K, and bands were visualized as above.

Analytic procedures

LDL and cell protein was assayed by the method of Lowry (27) in the presence of 0.05% sodium deoxycholate with BSA as the standard. Lipoprotein electrophoresis was done using the Titan gel lipoprotein electrophoresis system (Intermedico, Markham, Ontario). Lipoprotein bands were visualized by staining with Fat red.

Statistical analysis

Statistical analysis was done using ANOVA or Student's *t*-test as appropriate. $P < 0.05$ was taken as significant.

RESULTS

LOX-knockout mice

Homozygous LOX-1 deficient animals had no overt phenotype and were fertile. The absence of LOX-1 mRNA was verified by RT-PCR (**Fig. 1**).

Uptake of fluorescently labeled oxLDL by macrophages

The lipophilic fluorophore diI crosses lysosomal membranes very slowly and so serves as a cumulative marker of the quantity of labeled LDL that is internalized by cells (24, 28). To obtain a morphologic comparison of the internalization of oxLDL in control and LOX-1 deficient macrophages, we incubated peritoneal macrophages grown on coverslips for 5 h with diI-labeled oxLDL. Fluorescence micrographs indicate that there was no apparent difference in the intensity or distribution of fluorescence between wild-type and LOX-1 deficient cells (**Fig. 2**).

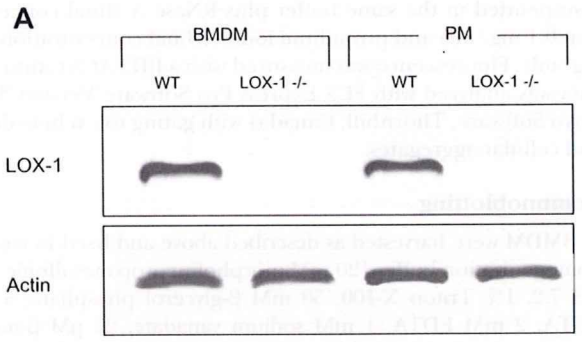

Fig. 1. Absence of LOX-1 mRNA in macrophages harvested from LOX-1 knockout mice. Absence of LOX-1 mRNA in knockout animals was verified by RT-PCR of total RNA from bone marrow derived macrophages (BMDM) or peritoneal macrophages (PM). An amplicon with migration consistent with the predicted nucleotide sequence is seen in the wild-type cells, whereas no band is seen in knockout cells.

Uptake and degradation of modified LDLs in wild-type and LOX-1 deficient peritoneal macrophages

To quantify the relative rates of oxLDL uptake, we incubated macrophages for 5 h with radioiodinated native LDL, oxLDL, or acetyl LDL and then measured rates of LDL uptake and degradation. There was no difference in the rate of uptake of native LDL or either modified LDL in wild-type compared with LOX-1 knockout peritoneal macrophages (**Fig. 3**).

Uptake and degradation of oxLDL in wild-type and LOX-1 deficient peritoneal macrophages

Different scavenger receptors are known to have different affinities for minimally, moderately, or extensively oxidized LDL. We therefore tested the uptake and degradation of radioactively labeled oxLDL in LOX-1 deficient and wild-type macrophages. There was no difference between wild-type and LOX-1 deficient macrophages in uptake or degradation of minimally, moderately, or extensively oxidized LDL (**Fig. 4**).

Effect of induction of LOX-1 gene expression on oxLDL uptake and degradation in wild-type macrophages

LOX-1 has been shown to mediate uptake and degradation of oxLDL in endothelial cells, smooth muscle cells, and in transfected cell lines. Hence, it seemed possible that the failure to detect a difference between wild-type and LOX-1 deficient macrophages might be because a high level of expression of SRAI/II and CD36 masked the contribution of LOX-1. To test this, we took advantage of the observation that lysophosphatidylcholine causes a marked and selective (up to 5-fold) induction of LOX-1 in endothelial cells and smooth muscle cells (29, 30). Cultured peritoneal macrophages from wild-type and LOX-1 deficient mice were preincubated for 12 h with varying concentrations of lysophosphatidylcholine, and then incubated for 5 h with ^{125}I oxLDL or ^{125}I LDL (**Fig. 5A**, 5B). Lysophosphatidylcholine caused a concentration-dependent increase in oxLDL uptake and degradation in wild-type macrophages but had no effect on uptake and

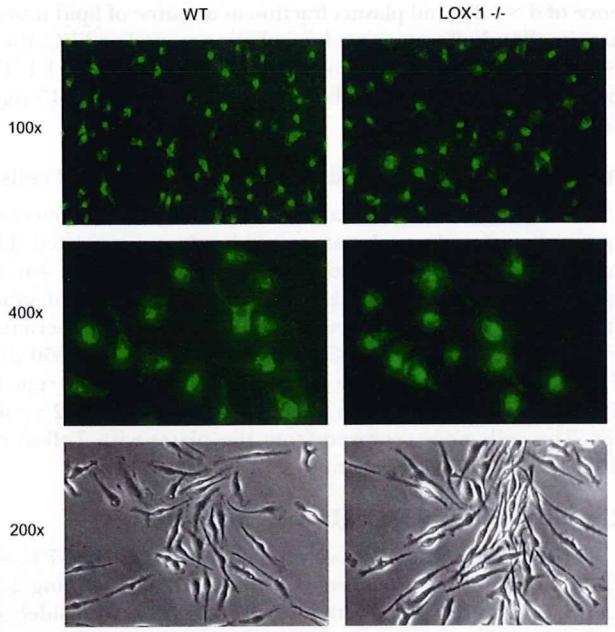

Fig. 2. Uptake of oxLDL in peritoneal macrophages. Resident peritoneal macrophages from wild-type (WT) and LOX-1 knockout mice were incubated for 5 h with 10μg/ml DiI-labeled oxidized LDL, and then examined using a Zeiss Axioskop fluorescence microscope. No difference in fluorescence intensity is seen.

degradation in LOX-1 deficient cells. These concentrations of lysophosphatidylcholine are the same as those reported to induce LOX-1 expression in smooth muscle cells and endothelial cells (29). The upregulation of LOX-1 mRNA by these concentrations of lysophosphatidylcholine was confirmed by RT-PCR (Fig. 5C).

In vivo clearance of oxLDL

To directly assess the role of LOX-1 in oxLDL clearance in vivo, we compared the rates at which oxLDL was removed from plasma from wild-type and LOX-1 deficient mice. Animals were injected first with ^{125}I-oxLDL and then

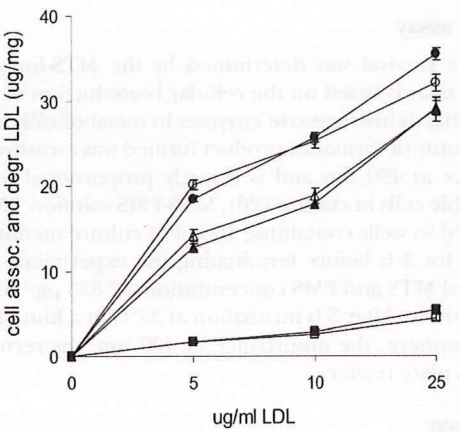

Fig. 3. Uptake and degradation of native, oxidized, and acetylated LDL in macrophages. Cultured peritoneal macrophages from wild-type mice (solid symbols) or knockout mice (open symbols) were incubated with the indicated concentration of ^{125}I-labeled native LDL, oxLDL, or acetyl LDL.

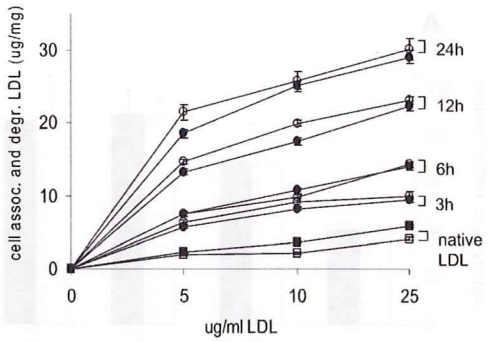

Fig. 4. Uptake and degradation of LDL oxidized to various degrees in wild-type and LOX-1 deficient peritoneal macrophages. Cultured peritoneal macrophages from wild-type mice (solid symbols) or knockout mice (open symbols) were incubated with the indicated concentration of native ^{125}I-LDL (squares) or ^{125}I-LDL oxidized by exposure to 5μM Cu^{2+} for 3 h, 6 h, 12 h, or 24 h (circles). The electrophoretic mobility of oxLDL was 1.0 (3 h), 1.3 (6 h), 2.2 (12 h) or 3.8 (24 h) times that of native LDL. After 5 h, cells and media were assayed for uptake and degradation of labeled lipoprotein. Results are the sum of cell-associated and degraded LDL expressed as μg LDL per mg cell protein. Values are the means +/− SEM of triplicates.

with native ^{125}I-LDL and serial blood samples were assayed for radioactivity. The rates of plasma clearance of oxLDL were very rapid and indistinguishable between wild-type and LOX-1 deficient animals (**Fig. 6**).

Role of LOX-1 in the ability of oxLDL to increase survival of BMDM

We have shown that oxLDL promotes growth and cytokine-independent survival in macrophages at least in part by activating the PI3K/PKB pro-survival pathway (15–17 26). We previously found that oxLDL promoted survival in SRAI/II-deficient macrophages (31) and in CD36-deficient macrophages (unpublished), so we hypothesized that LOX-1 might be the receptor required for PKB activation. To address this, we compared the ability of oxLDL to promote survival in cytokine-deprived BMDM from wild-type and LOX-1 deficient mice. After 24 h there was no significant difference in the viability of wild-type and LOX-1 deficient cells treated with oxLDL (**Fig. 7A**). There was no significant difference between wild-type and LOX-1 BMDM in the percentage of sub-diploid cells after incubation with oxLDL (Fig. 7B). Deficiency of LOX-1 did not abolish the ability of oxLDL to promote PKB phosphorylation in BMDM (**Fig. 8**).

DISCUSSION

The studies described in this report address two different aspects of the interaction of oxLDL with LOX-1 in macrophages. The first issue is the role of LOX-1 in uptake and degradation of oxLDL by macrophages. LOX-1 clearly has the ability to bind and internalize LDL in endothelial cells and in CHO cells transfected with LOX-1 receptor constructs (3). LOX-1 has a similar ligand specificity as SR-AI/II and CD36, although its affinity for ox-

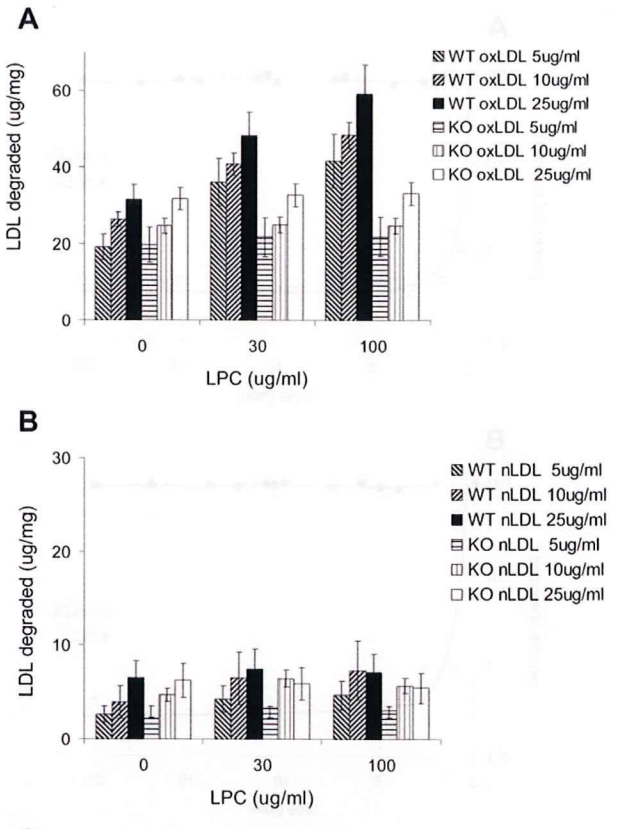

Fig. 5. Effect of induction of LOX-1 with lysophosphatidylcholine on oxLDL uptake and degradation. Cultured peritoneal macrophages from wild-type and LOX-1 knockout mice were preincubated for 12 h with 0, 30, or 100 ug/ml lysophosphatidylcholine. Cells were then washed and incubated for 5 h with varying concentrations of ^{125}I-oxLDL (A) or ^{125}I-LDL (B). Values shown are means ± SD of the sum of cell-associated and degraded oxLDL, reflecting total oxLDL uptake during the incubation. (C) RT-PCR blot showing that LOX-1 mRNA expression was increased in wild-type macrophages by these concentrations of lysophosphatidylcholine.

LDL is substantially higher than its affinity for acetyl LDL (31). We previously showed that about 70% of the uptake of oxLDL in macrophages was not due to SRAI/II (12). Competition experiments indicated that polyinosinic acid, but not acetyl LDL or native LDL, blocked the SRAI/II-independent uptake of oxidized LDL (12). Although CD36 has been shown to contribute to oxLDL uptake in macrophages, our preliminary findings in CD36 −/− macrophages showed no reduction in the anti-apoptotic effect of oxLDL. Hence it seemed possible that some of the SRAI/II and CD36-independent uptake might be due to a receptor such as LOX-1. This receptor has a reported

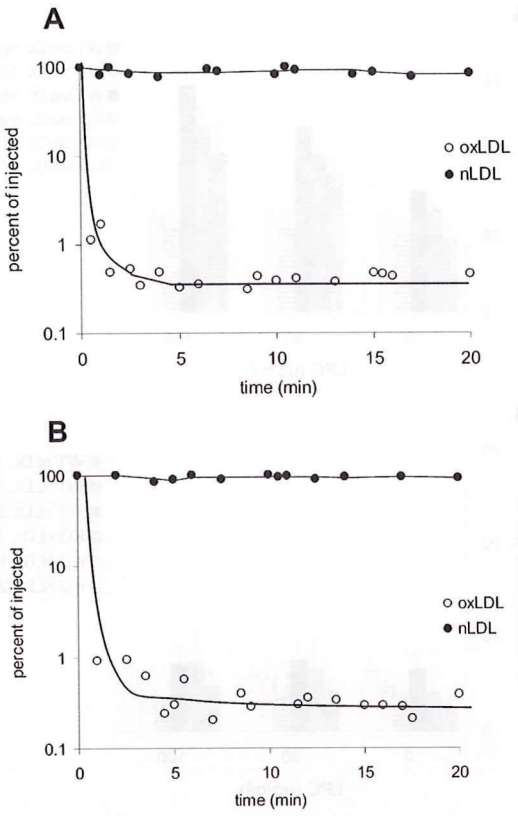

Fig. 6. In vivo plasma clearance of oxidized and native LDL in wild-type and LOX-1 deficient mice. Wild-type mice (A, n = 3) or LOX-1 knockout mice (B, n = 3) were anesthetized with 2% isoflurane. Oxidized ^{125}I LDL (open circles) or native ^{125}I LDL (solid circles) was injected through a cannula placed in the internal jugular vein. Serial 20 μl blood samples were withdrawn at the indicated time points and radioactivity was measured. Points for all three animals in each case are plotted together. The electrophoretic mobility of oxLDL in this experiment was 4.1-fold that of native LDL.

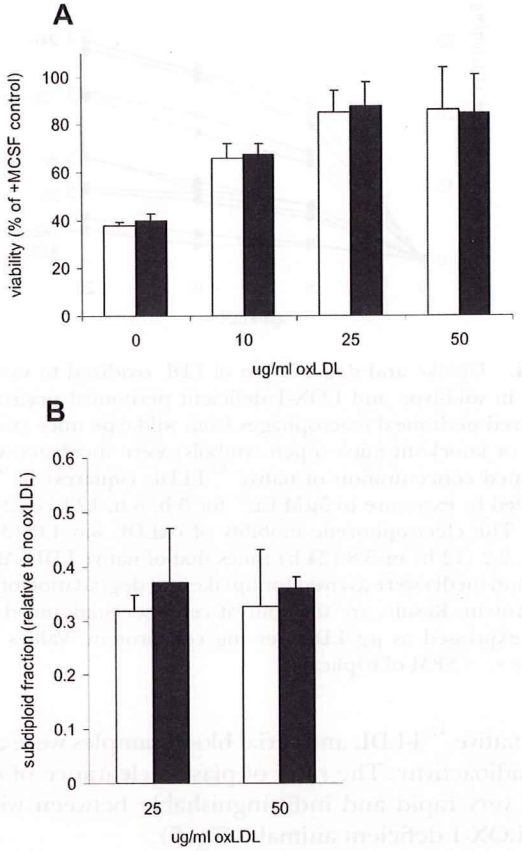

Fig. 7. LOX-1 deficiency does not impair the ability of oxLDL to inhibit macrophage apoptosis. (A) BMDM from wild-type mice (open bars) or LOX-1 −/− mice (solid bars) were seeded at 3 × 10^3 cells/well in 96 well plates and cultured for 24 h. They were then washed and incubated for 24 h without M-CSF but with the indicated concentrations of ox-LDL. Viability was then measured by the bioreduction of MTS (described in Materials and Methods) and expressed as a percentage of that in control cells treated with M-CSF. (B) BMDM were plated at 10^6 cells/well in six well plates and incubated for 24 h in medium containing indicated concentration of oxLDL but no M-CSF. The sub-diploid population was measured by flow cytometry after propidium iodide staining. Results are expressed relative to control cells incubated without CSF, which typically amounted to about 40% of cells. In both panels, results are the means ± SD of pooled data from three independent experiments. None of the differences between wild-type and LOX-1 −/−. macrophages was significant.

ligand specificity that is congruent with the ligand specificity that we observed in SRAI/II-deficient macrophages (12). It has been shown that LOX-1 is expressed in monocyte-derived macrophages (14) and in macrophages in atherosclerotic lesions (7). Furthermore, a recent report indicates that LOX-1 accounts for at least half the uptake of oxLDL in PMA-activated HL-60 macrophages (32). However, in the present studies there was no effect of LOX-1 gene inactivation on oxLDL uptake by BMDM or peritoneal macrophages.

One assumption that is implicit in the interpretation of our results is that there is no compensatory increase in the activity of other scavenger receptors in LOX-1 −/− mice and macrophages that exactly balances the effect of the inactivation of LOX-1 gene. A minor contribution of LOX-1 to oxLDL uptake might be masked if there was a high level of nonsaturable uptake mediated by phagocytosis or pinocytosis. However, we have previously shown that at the relatively low concentration of labeled oxLDL used in the present studies, more than 80% of the uptake and degradation of the labeled oxLDL can be competed by 10-fold excess of unlabeled oxLDL or by polyinosinic acid, indicating that the uptake is mediated by a high-affinity saturable mechanism, presumably a receptor(s) (12, 33). Overall, our finding that LOX-1 gene inactivation does not significantly alter oxLDL uptake in unstimulated murine macrophages indicates that LOX-1 accounts for at most 5–10% of oxLDL uptake by these cells. On the other hand, when LOX-1 was upregulated in macrophages by preincubation with lysophosphatidylcholine, internalization of ox-LDL increased by more than 40%. It has been shown that pro-inflammatory cytokines such as TNFα (34) and TGFβ (35) upregulate LOX-1 and downregulate SR-AI/II and CD36. Hence, it is possible that in microenvironments where these cytokines are relatively abundant, notably in atherosclerotic lesions, LOX-1 might play a significant role in oxLDL uptake. It is also possible that endothelial cells and smooth muscle cells might rely on LOX-1 as a recep-

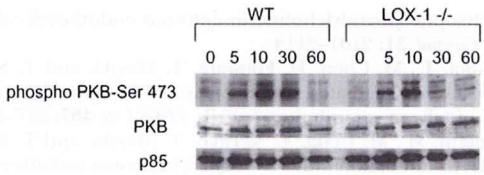

Fig. 8. LOX-1 is not essential for induction of PKB phosphorylation by oxLDL in BMDM. Bone marrow-derived macrophages from wild-type (WT) or LOX-1 knockout mice were incubated with or without 25 μg/ml oxLDL for 0–60 min. Cell lysates were then analyzed by immunoblotting for phosphorylation of PKB at serine 473. Immunostaining for the p85 subunit of PI3K as well as for total PKB was used to monitor loading.

tor for the internalization of oxLDL or for mediating oxLDL-induced signal transduction.

The second issue addressed by these studies was the potential role of LOX-1 in survival signaling. The importance of macrophage survival has been recently underlined by a series of studies in different animal models. Currently it is believed that at least in early stages of atherosclerosis, inhibition of macrophage apoptosis or induction of macrophage growth enhances lesion progression (36). It has been shown that oxLDL activates p42/44 MAPK (15), p38MAPK (37), PKC (38), and PI3K/PKB (15, 26). Activation of PI3K/PKB by oxidized LDL promotes growth and survival of macrophages (15, 26). The upstream steps by which oxLDL activates these signaling pathways have not yet been defined. As LOX-1 has been shown to activate PKCα (39), PKCβ (40), p38MAPK (41), and p42/44MAPK (42), it seemed appropriate to determine if it accounted for part of the anti-apoptotic signaling of oxLDL. However, we found no difference in the anti-apoptotic effect of oxLDL in LOX-1 knockout compared with wild-type macrophages.

In contrast to our findings in BMDM, previous studies in smooth muscle cells (10), cultured endothelial cells (43), and chondrocytes (44) reported a pro-apoptotic effect of oxLDL acting at least in part via LOX-1. There are a number of explanations for these apparently discrepant results. In the study by Kataoka et al. in smooth muscle cells (10), oxLDL only induced apoptosis at concentrations of 40 μg/ml or higher, and Fig. 1A in that paper actually shows increased viability of smooth muscle cells at lower concentrations of oxLDL. Also, they incubated cells in medium containing only 1% fetal bovine serum. We have reported a similar biphasic effect of oxLDL in macrophages, with concentrations higher than 100 μg/ml associated with toxicity in macrophages incubated in 10% fetal bovine serum (15). In macrophages incubated in serum-free medium, the threshold for toxicity of oxLDL was much lower, around 20 μg/ml (15). The study by Imanishi and colleagues found that oxLDL upregulated Fas expression and potentiated the effect of an agonistic anti-Fas antibody on apoptosis in endothelial cells (43). This study did not investigate apoptosis induced by oxLDL, only its effect on apoptosis induced by anti-Fas. In this study, endothelial cells were cultured in medium containing only 1% FBS, which would have made them more vulnerable to toxic effects of oxLDL. The study by Nakagawa and coworkers showed that in chondrocytes, oxLDL at concentrations of 40 μg/ml or higher induced apoptosis. Chondrocytes were incubated in serum-free medium, which may explain why the toxic threshold for oxLDL was relatively low. Also, their oxLDL preparations may not have been dialyzed after oxidation, and we have previously shown that this results in a high concentration of toxic water-soluble aldehydes in the oxLDL mixture (45) Although, it appears that LOX-1 plays a role in oxLDL-mediated toxicity in these cells, our results in macrophages provide no evidence that LOX-1 is involved in the anti-apoptotic effect of low concentrations of oxLDL.

Other receptors that are capable of binding oxLDL or some of its components could play a role in pro-survival signaling, including the phosphatidylserine receptor (46), PPARα (47, 48), PPARγ (49–51), TLR4 (52), and FcγRII (53). Studies are under way to determine if any of these play a role in the pro-survival effect of oxLDL in macrophages.

Dr. Osamu Cynshi provided LOX-1 knockout mice from a colony maintained at Chugai Pharmaceutical Corp., Tokyo.

REFERENCES

1. Moriwaki, H., N. Kume, T. Sawamura, T. Aoyama, H. Hoshikawa, H. Ochi, E. Nishi, T. Masaki, and T. Kita. 1998. Ligand specificity of LOX-1, a novel endothelial receptor for oxidized low density lipoprotein. *Arterioscler. Thromb. Vasc. Biol.* **18:** 1541–1547.
2. Chen, M., T. Masaki, and T. Sawamura. 2002. LOX-1, the receptor for oxidized low-density lipoprotein identified from endothelial cells: implications in endothelial dysfunction and atherosclerosis. *Pharmacol. Ther.* **95:** 89–100.
3. Sawamura, T., N. Kume, T. Aoyama, H. Moriwaki, H. Hoshikawa, Y. Aiba, T. Tanaka, S. Miwa, Y. Katsura, T. Kita, et al. 1997. An endothelial receptor for oxidized low-density lipoprotein. *Nature.* **386:** 73–77.
4. Cominacini, L., A. F. Pasini, U. Garbin, A. Davoli, M. L. Tosetti, M. Campagnola, A. Rigoni, A. M. Pastorino, V. Lo Cascio, and T. Sawamura. 2000. Oxidized low density lipoprotein (ox-LDL) binding to ox-LDL receptor-1 in endothelial cells induces the activation of NF-kappaB through an increased production of intracellular reactive oxygen species. *J. Biol. Chem.* **275:** 12633–12638.
5. Cominacini, L., A. Rigoni, A. F. Pasini, U. Garbin, A. Davoli, M. Campagnola, A. M. Pastorino, V. Lo Cascio, and T. Sawamura. 2001. The binding of oxidized low density lipoprotein (ox-LDL) to ox-LDL receptor-1 reduces the intracellular concentration of nitric oxide in endothelial cells through an increased production of superoxide. *J. Biol. Chem.* **276:** 13750–13755.
6. Li, D., and J. Mehta. 2000. Upregulation of endothelial receptor for oxidized LDL (LOX-1) by oxidized LDL and implications in apoptosis of human coronary artery endothelial cells. Evidence from use of antisense LOX-1 mRNA and chemical inhibitors. *Arterioscler. Thromb. Vasc. Biol.* **20:** 1116–1122.
7. Kataoka, H., N. Kume, S. Miyamoto, M. Minami, H. Moriwaki, T. Murase, T. Sawamura, T. Masaki, N. Hashimoto, and T. Kita. 1999. Expression of lectinlike oxidized low-density lipoprotein receptor-1 in human atherosclerotic lesions. *Circulation.* **99:** 3110–3117.
8. Chen, C. H., W. Jiang, D. P. Via, S. Luo, T. R. Li, Y. T. Lee, and P. D. Henry. 2000. Oxidized low-density lipoproteins inhibit endothelial cell proliferation by suppressing basic fibroblast growth factor expression. *Circulation.* **101:** 171–177.
9. Mehta, J. L., N. Sanada, C. P. Hu, J. Chen, A. Dandapat, F. Sugawara, H. Satoh, K. Inoue, Y. Kawase, K. Jishage, et al. 2007. Deletion of LOX-1 reduces atherogenesis in LDLR knockout mice fed high cholesterol diet. *Circ. Res.* **100:** 1634–1642.

10. Kataoka, H., N. Kume, S. Miyamoto, M. Minami, M. Morimoto, K. Hayashida, N. Hashimoto, and T. Kita. 2001. Oxidized LDL modulates Bax/Bcl-2 through the lectinlike Ox-LDL receptor-1 in vascular smooth muscle cells. *Arterioscler. Thromb. Vasc. Biol.* **21:** 955–960.
11. Greaves, D. R., and S. Gordon. 2005. Thematic review series: The immune system and atherogenesis. Recent insights into the biology of macrophage scavenger receptors. *J. Lipid Res.* **46:** 11–20.
12. Lougheed, M., C. Ming Lum, W. Ling, H. Suzuki, T. Kodama, and U. P. Steinbrecher. 1997. High-affinity saturable uptake of oxidized low density lipoprotein by macrophages from mice lacking the scavenger receptor class A type I/II. *J. Biol. Chem.* **272:** 12938–12944.
13. Kunjathoor, V. V., M. Febbraio, E. A. Podrez, K. J. Moore, L. Andersson, S. Koehn, J. S. Rhee, R. Silverstein, H. F. Hoff, and M. W. Freeman. 2002. Scavenger receptors class A-I/II and CD36 are the principal receptors responsible for the uptake of modified low density lipoprotein leading to lipid loading in macrophages. *J. Biol. Chem.* **277:** 49982–49988.
14. Yoshida, H., N. Kondratenko, S. Green, D. Steinberg, and O. Quehenberger. 1998. Identification of the lectin-like receptor for oxidized low-density lipoprotein in human macrophages and its potential role as a scavenger receptor. *Biochem. J.* **334:** 9–13.
15. Hundal, R., B. Salh, J. Schrader, A. Gómez-Muñoz, V. Duronio, and U. Steinbrecher. 2001. Oxidized low density lipoprotein inhibits macrophage apoptosis through activation of the PI 3-kinase/PKB pathway. *J. Lipid Res.* **42:** 1483–1491.
16. Hundal, R., A. Gómez-Muñoz, J. Kong, B. Salh, A. Marotta, V. Duronio, and U. Steinbrecher. 2003. Oxidized low density lipoprotein inhibits macrophage apoptosis by blocking ceramide generation, thereby maintaining PKB activation and Bcl-XL levels. *J. Biol. Chem.* **278:** 24399–24408.
17. Martens, J., M. Lougheed, A. Gomez-Muñoz, and U. Steinbrecher. 1999. A modification of apolipoprotein B accounts for most of the induction of macrophage growth by oxidized low density lipoprotein. *J. Biol. Chem.* **274:** 10903–10910.
18. Matsunaga, T., S. Hokari, I. Koyama, T. Harada, and T. Komoda. 2003. NF-kappa B activation in endothelial cells treated with oxidized high-density lipoprotein. *Biochem. Biophys. Res. Commun.* **303:** 313–319.
19. Havel, R. J., H. A. Eder, and J. H. Bragdon. 1955. The distribution and chemical composition of ultracentrifugally separated lipoproteins in human serum. *J. Clin. Invest.* **43:** 1345–1353.
20. Bilheimer, D. W., S. Eisenberg, and R. I. Levy. 1972. The metabolism of very low density lipoproteins. *Biochim. Biophys. Acta.* **260:** 212–221.
21. Steinbrecher, U. P. 1987. Oxidation of human low density lipoproteins results in derivatization of lysine residues of apolipoprotein B by lipid peroxide decomposition products. *J. Biol. Chem.* **262:** 3603–3608.
22. Zhang, H., Y. Yang, and U. P. Steinbrecher. 1993. Structural requirements for the binding of modified proteins to the scavenger receptor of macrophages. *J. Biol. Chem.* **268:** 5535–5542.
23. Hamilton, J. A., D. Myers, W. Jessup, F. Cochrane, R. Byrne, G. Whitty, and S. Moss. 1999. Oxidized LDL can induce macrophage survival, DNA synthesis, and enhanced proliferative response to CSF-1 and GM-CSF. *Arterioscler. Thromb. Vasc. Biol.* **19:** 98–105.
24. Pitas, R. E., T. L. Innerarity, J. N. Weinstein, and R. W. Mahley. 1981. Acetoacetylated lipoproteins used to distinguish fibroblasts from macrophages in vitro by fluorescence microscopy. *Arteriosclerosis.* **1:** 177–185.
25. Ling, W., M. Lougheed, H. Suzuki, A. Buchan, T. Kodama, and U. Steinbrecher. 1997. Oxidized or acetylated low density lipoprotein are rapidly cleared by the liver in mice with disruption of the scavenger receptor class A type I/type II gene. *J. Clin. Invest.* **100:** 244–252.
26. Martens, J., N. Reiner, P. Herrera-Velit, and U. Steinbrecher. 1998. Phosphatidylinositol 3-kinase is involved in the induction of macrophage growth by oxidized low density lipoprotein. *J. Biol. Chem.* **273:** 4915–4920.
27. Lowry, O. H., N. J. Rosebrough, A. L. Farr, and R. J. Randall. 1951. Protein measurement with the Folin phenol reagent. *J. Biol. Chem.* **193:** 265–275.
28. Stephan, Z., and E. Yurachek. 1993. Rapid fluorometric assay of LDL receptor activity by DiI-labelled LDL. *J. Lipid Res.* **34:** 325–330.
29. Aoyama, T., H. Fujiwara, T. Masaki, and T. Sawamura. 1999. Induction of lectin-like oxidized LDL receptor by oxidized LDL and lysophosphatidylcholine in cultured endothelial cells. *J. Mol. Cell. Cardiol.* **31:** 2101–2114.
30. Aoyama, T., M. Chen, H. Fujiwara, T. Masaki, and T. Sawamura. 2000. LOX-1 mediates lysophosphatidylcholine-induced oxidized LDL uptake in smooth muscle cells. *FEBS Lett.* **467:** 217–220.
31. Kakutani, M., M. Ueda, T. Naruko, T. Masaki, and T. Sawamura. 2001. Accumulation of LOX-1 ligand in plasma and atherosclerotic lesions of Watanabe heritable hyperlipidemic rabbits: identification by a novel enzyme immunoassay. *Biochem. Biophys. Res. Commun.* **282:** 180–185.
32. Smirnova, I. V., M. Kajstura, T. Sawamura, and M. S. Goligorsky. 2004. Asymmetric dimethylarginine upregulates LOX-1 in activated macrophages: role in foam cell formation. *Am. J. Physiol. Heart Circ. Physiol.* **287:** H782–H790.
33. Lougheed, M., and U. P. Steinbrecher. 1996. Mechanism of uptake of copper-oxidized low density lipoprotein in macrophages is dependent on its extent of oxidation. *J. Biol. Chem.* **271:** 11798–11805.
34. Kume, N., H. Moriwaki, H. Kataoka, M. Minami, T. Murase, T. Sawamura, T. Masaki, and T. Kita. 2000. Inducible expression of LOX-1, a novel receptor for oxidized LDL, in macrophages and vascular smooth muscle cells. *Ann. N. Y. Acad. Sci.* **902:** 323–327.
35. Draude, G., and R. L. Lorenz. 2000. TGF-beta1 downregulates CD36 and scavenger receptor A but upregulates LOX-1 in human macrophages. *Am. J. Physiol. Heart Circ. Physiol.* **278:** H1042–H1048.
36. Tabas, I. 2005. Consequences and therapeutic implications of macrophage apoptosis in atherosclerosis: the importance of lesion stage and phagocytic efficiency. *Arterioscler. Thromb. Vasc. Biol.* **25:** 2255–2264.
37. Salomonsson, L., S. Pettersson, M. C. Englund, O. Wiklund, and B. G. Ohlsson. 2002. Post-transcriptional regulation of VEGF expression by oxidised LDL in human macrophages. *Eur. J. Clin. Invest.* **32:** 767–774.
38. Claus, R., B. Fyrnys, H. P. Deigner, and G. Wolf. 1996. Oxidized low-density lipoprotein stimulates protein kinase C (PKC) and induces expression of PKC-isotypes via prostaglandin-H-synthase in P388D1 macrophage-like cells. *Biochemistry.* **35:** 4911–4922.
39. Li, D., L. Liu, H. Chen, T. Sawamura, and J. L. Mehta. 2003. LOX-1, an oxidized LDL endothelial receptor, induces CD40/CD40L signaling in human coronary artery endothelial cells. *Arterioscler. Thromb. Vasc. Biol.* **23:** 816–821.
40. Li, D., L. Liu, H. Chen, T. Sawamura, S. Ranganathan, and J. L. Mehta. 2003. LOX-1 mediates oxidized low-density lipoprotein-induced expression of matrix metalloproteinases in human coronary artery endothelial cells. *Circulation.* **107:** 612–617.
41. Iwai-Kanai, E., K. Hasegawa, T. Sawamura, M. Fujita, T. Yanazume, S. Toyokuni, S. Adachi, Y. Kihara, and S. Sasayama. 2001. Activation of lectin-like oxidized low-density lipoprotein receptor-1 induces apoptosis in cultured neonatal rat cardiac myocytes. *Circulation.* **104:** 2948–2954.
42. Li, D., and J. L. Mehta. 2000. Antisense to LOX-1 inhibits oxidized LDL-mediated upregulation of monocyte chemoattractant protein-1 and monocyte adhesion to human coronary artery endothelial cells. *Circulation.* **101:** 2889–2895.
43. Imanishi, T., T. Hano, T. Sawamura, S. Takarada, and I. Nishio. 2002. Oxidized low density lipoprotein potentiation of Fas-induced apoptosis through lectin-like oxidized-low density lipoprotein receptor-1 in human umbilical vascular endothelial cells. *Circ. J.* **66:** 1060–1064.
44. Nakagawa, T., T. Yasuda, H. Hoshikawa, M. Shimizu, T. Kakinuma, M. Chen, T. Masaki, T. Nakamura, and T. Sawamura. 2002. LOX-1 expressed in cultured rat chondrocytes mediates oxidized LDL-induced cell death-possible role of dephosphorylation of Akt. *Biochem. Biophys. Res. Commun.* **299:** 91–97.
45. Steinbrecher, U. P., A. Gomez-Munoz, and V. Duronio. 2004. Acid sphingomyelinase in macrophage apoptosis. *Curr. Opin. Lipidol.* **15:** 531–537.
46. Fadok, V. A., D. Xue, and P. Henson. 2001. If phosphatidylserine is the death knell, a new phosphatidylserine-specific receptor is the bellringer. *Cell Death Differ.* **8:** 582–587.
47. Delerive, P., C. Furman, E. Teissier, J. Fruchart, P. Duriez, and B. Staels. 2000. Oxidized phospholipids activate PPARalpha in a phospholipase A2-dependent manner. *FEBS Lett.* **471:** 34–38.
48. Lee, H., W. Shi, P. Tontonoz, S. Wang, G. Subbanagounder, C. C. Hedrick, S. Hama, C. Borromeo, R. M. Evans, J. A. Berliner, et al. 2000. Role for peroxisome proliferator-activated receptor alpha in oxidized phospholipid-induced synthesis of monocyte chemotac-

tic protein-1 and interleukin-8 by endothelial cells. *Circ. Res.* **87:** 516–521.
49. Nagy, L., P. Tontonoz, J. Alvarez, H. Chen, and R. Evans. 1998. Oxidized LDL regulates macrophage gene expression through ligand activation of PPARg. *Cell.* **93:** 229–240.
50. Davies, S. S., A. V. Pontsler, G. K. Marathe, K. A. Harrison, R. C. Murphy, J. C. Hinshaw, G. D. Prestwich, A. S. Hilaire, S. M. Prescott, G. A. Zimmerman, et al. 2001. Oxidized alkyl phospholipids are specific, high affinity peroxisome proliferator-activated receptor gamma ligands and agonists. *J. Biol. Chem.* **276:** 16015–16023.
51. Pontsler, A. V., A. St Hilaire, G. K. Marathe, G. A. Zimmerman, and T. M. McIntyre. 2002. Cyclooxygenase-2 is induced in monocytes by peroxisome proliferator activated receptor gamma and oxidized alkyl phospholipids from oxidized low density lipoprotein. *J. Biol. Chem.* **277:** 13029–13036.
52. Miller, Y. I., S. Viriyakosol, C. J. Binder, J. R. Feramisco, T. N. Kirkland, and J. L. Witztum. 2003. Minimally modified LDL binds to CD14, induces macrophage spreading via TLR4/MD-2, and inhibits phagocytosis of apoptotic cells. *J. Biol. Chem.* **278:** 1561–1568.
53. Stanton, L. W., R. T. White, C. M. Bryant, A. A. Protter, and G. Endemann. 1992. A macrophage Fc receptor for IgG is also a receptor for oxidized low density lipoprotein. *J. Biol. Chem.* **267:** 22446–22451.

Cardiovascular Research (2009) 84, 127–136
doi:10.1093/cvr/cvp177

LOX-1-MT1-MMP axis is crucial for RhoA and Rac1 activation induced by oxidized low-density lipoprotein in endothelial cells

Koichi Sugimoto[1], Toshiyuki Ishibashi[1]*, Tatsuya Sawamura[2,3], Nobutaka Inoue[2], Masashi Kamioka[1], Hironori Uekita[1], Hiroshi Ohkawara[1], Takayuki Sakamoto[1], Nobuo Sakamoto[1], Yasuo Okamoto[4], Yoh Takuwa[4], Akemi Kakino[2], Yoshiko Fujita[2], Takeshi Tanaka[3], Tamio Teramoto[5], Yukio Maruyama[1,6], and Yasuchika Takeishi[1]

[1]*First Department of Internal Medicine, Fukushima Medical University, 1 Hikarigaoka, Fukushima 960-1295, Japan;* [2]*Department of Bioscience, National Cardiovascular Center Research Institute, Osaka, Japan;* [3]*International Research and Educational Institute for Integrated Medical Sciences, Tokyo Women's University, Tokyo, Japan;* [4]*Department of Physiology, Kanazawa University Graduate School of Medicine, Kanazawa, Japan;* [5]*Department of Internal Medicine, Teikyo University School of Medicine, Tokyo, Japan; and* [6]*Hoshi General Hospital, Fukushima, Japan*

Received 14 October 2008; revised 8 May 2009; accepted 26 May 2009; online publish-ahead-of-print 1 June 2009

Time for primary review: 25 days

KEYWORDS
LOX-1;
MT1-MMP;
RhoA;
Rac1;
Endothelial dysfunction

Aims RhoA and Rac1 activation plays a key role in endothelial dysfunction. Lectin-like oxidized low-density lipoprotein receptor-1 (LOX-1) is a major receptor for oxidized low-density lipoprotein (ox-LDL) in endothelial cells (ECs). Membrane type 1 matrix metalloproteinase (MT1-MMP) has been shown to be involved in atherogenesis. This study was conducted to investigate the role of the LOX-1-MT1-MMP axis in RhoA and Rac1 activation in response to ox-LDL in ECs.

Methods and results Ox-LDL induced rapid RhoA and Rac1 activation as well as MT1-MMP activity in cultured human aortic ECs. Inhibition of LOX-1 prevented ox-LDL-dependent RhoA and Rac1 activation. Knockdown of MT1-MMP by small interfering RNA prevented ox-LDL-induced RhoA and Rac1 activation, indicating that MT1-MMP is upstream of RhoA and Rac1. Fluorescent immunostaining revealed the colocalization of LOX-1 and MT1-MMP, and the formation of a complex of LOX-1 with MT1-MMP was detected by immunoprecipitation. Blockade of LOX-1 or MT1-MMP prevented RhoA-dependent endothelial NO synthase protein downregulation and cell invasion, Rac1-mediated NADPH oxidase activity, and reactive oxygen species generation.

Conclusion The present study provides evidence that the LOX-1-MT1-MMP axis plays a crucial role in RhoA and Rac1 activation signalling pathways in ox-LDL stimulation, suggesting that this axis may be a promising target for treating endothelial dysfunction.

1. Introduction

Endothelial dysfunction is crucial for the initiation and development of atherosclerosis.[1,2] Oxidized low-density lipoprotein (ox-LDL) impairs endothelial function, giving rise to reactive oxygen species (ROS) generation, and reduced nitric oxide (NO) production.[1,2] It is widely acknowledged that ox-LDL downregulates the expression of endothelial nitric oxide synthase (eNOS), which is associated with the activation of small GTP-binding protein, RhoA.[3] Earlier, we reported that lysophosphatidylcholine, a phospholipid compound of ox-LDL, activates RhoA within 1 min in cultured human aortic endothelial cells (HAECs).[4] These observations indicate that rapid RhoA activation plays a pivotal role in the downregulation of eNOS induced by ox-LDL. Ox-LDL-triggered ROS generation is predominantly mediated via NADPH oxidase in the vasculature, and small GTP-binding protein Rac1 is a component of NADPH oxidase,[2,5–7] indicating that Rac1 is critical for ox-LDL-stimulated ROS generation via NADPH oxidase in ECs. Lectin-like ox-LDL receptor-1 (LOX-1) with a type II membrane protein structure has been identified as a major endothelial receptor for ox-LDL in endothelial cells (ECs).[8] Thus, an ox-LDL-LOX-1 axis appears to be crucial for the pathogenesis of endothelial dysfunction in coronary artery disease. However, there is no report indicating that LOX-1 forms a complex with other molecule(s).

Degradation of the vascular extracellular matrix by secreted and membrane type matrix metalloproteinases

* Corresponding author. Tel: +81 24 547 1190; fax: +81 24 548 1821.
E-mail address: masaishi@fmu.ac.jp

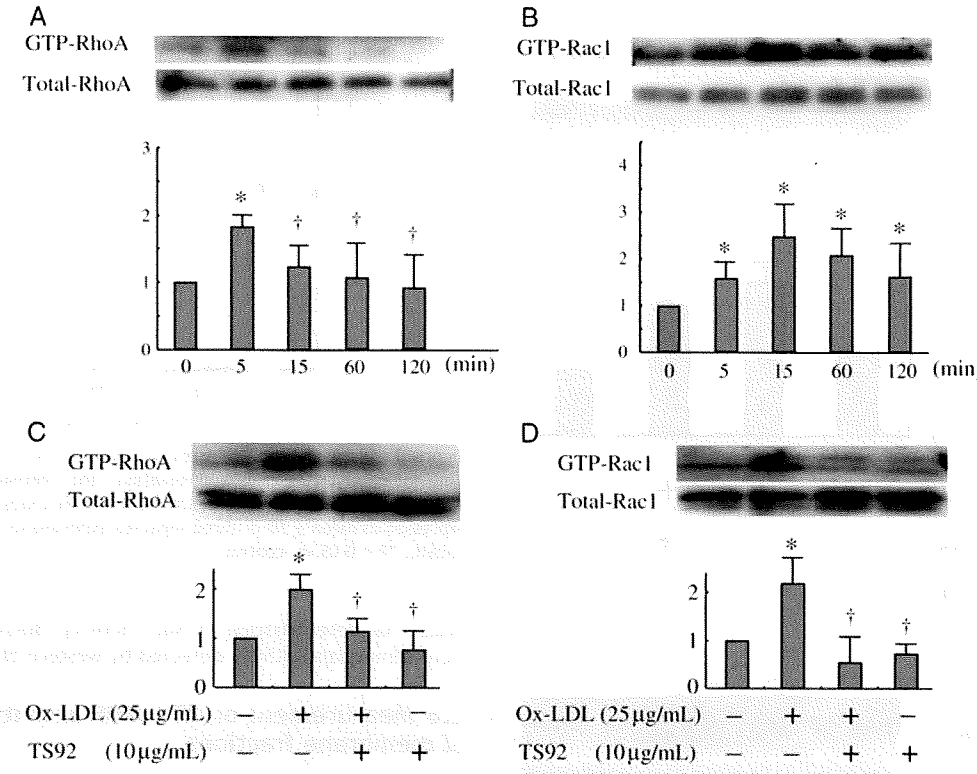

Figure 1 Role of LOX-1 in ox-LDL-triggered RhoA and Rac1 activation. (*A*, *B*) Levels of GTP-bound active forms of RhoA and Rac1 as determined by pull-down assays in cultured human aortic endothelial cells (HAECs) 5–120 min after adding 25 μg/mL ox-LDL. (*C*, *D*) Effects of inhibition of LOX-1 on ox-LDL-induced GTP/GDP exchange (GTP-loading) of RhoA and Rac1. TS92 (10 μg/mL), a monoclonal antibody to LOX-1, was added to HAECs 60 min before adding ox-LDL. The GTP-loading of RhoA and Rac1 was determined by pull-down assays after 5 and 15 min of ox-LDL stimulation, respectively. Quantitative results of GTP-RhoA and GTP-Rac1 were normalized by total RhoA or Rac1 levels. Bars are mean ± SD of quantitative densitometric analyses from three separate experiments. Representative immunoblots are shown at the top. $^{*}P < 0.05$ vs. control; $^{\dagger}P < 0.05$ vs. ox-LDL.

(secreted MMPs and MT-MMPs) plays an important role in smooth muscle cell migration and invasion and plaque instability, which in turn, contribute to the pathogenesis of coronary artery disease, especially acute coronary syndromes.[9] Ox-LDL has been shown to increase the expression and activities of MMPs including secreted MMPs and MT-MMPs.[10,11] MT-MMPs possess transmembrane and cytoplasmic domains in addition to extracellular domains. The activities of secreted MMPs and MT-MMPs are modulated by the tissue inhibitor of metalloproteinases (TIMPs). MT-MMPs are inhibited by TIMP-2, whereas TIMP-1 and TIMP-2 inhibit secreted MMPs. Membrane type 1 MMP (MT1-MMP) participates in skeletal development, cell growth, and angiogenesis.[12,13] MT1-MMP also has been shown to play a role in cell migration and invasion mediated via the Rho family of GTPases such as Rho, Rac, and Cdc42.[14–16]

In the present study, we hypothesized that MT1-MMP plays an integral role in ox-LDL-triggered RhoA and Rac1 signalling pathways and that MT1-MMP and LOX-1 may form a complex.

2. Methods

The investigation conforms with the principles outlined in the Declaration of Helsinki.[17]

2.1 Materials

The sources of most of the conventional reagents were described previously.[18,19] Recombinant human TIMP-1 and TIMP-2 were obtained from DAIICHI Fine Chemical Co., Ltd (Toyama, Japan). Neutralizing antibody to LOX-1, TS92, was used for the inhibition of LOX-1.[10] Diphenyleneiodonium (DPI), a selective NADPH oxidase inhibitor, was from Sigma-Aldrich Co. (St Louis, MO, USA) and C3 exoenzyme, a Rho inhibitor, from Upstate Biotechnology (Lake Placid, NY, USA).

2.2 Preparation of ECs

HAECs were cultured according to the suppliers' instructions (Clonetics Inc., Walkersville, MD, USA and Sanko Junyaku Co., Ltd, Tokyo, Japan) and used for all experiments after 5–10 passages.[4,20]

2.3 Preparation of ox-LDL

Human LDL was isolated from the serum of fasting normolipidaemic volunteers by sequential ultracentrifugation and ox-LDL was prepared by incubating native LDL for 24 h at 4°C in phosphate-buffered saline (PBS) containing 5 μmol/L $CuSO_4$, and then extensively dialyzed against PBS and sterilized by filtration as described previously.[21]

2.4 Western blotting

The expression of RhoA, Rac1, eNOS, and α-tubulin was determined by western blotting.[4,20,22] For immunoblotting, we used mouse monoclonal antibodies to RhoA (Santa Cruz Biotechnology, Santa Cruz, CA, USA) and Rac1 (Upstate Biotechnology) diluted 1:500, and to eNOS (Transduction Laboratories, Lexington, KY, USA) diluted 1:1000 and α-tubulin (Santa Cruz Biotechnology) diluted 1:500. The signals from immunoreactive bands were visualized by

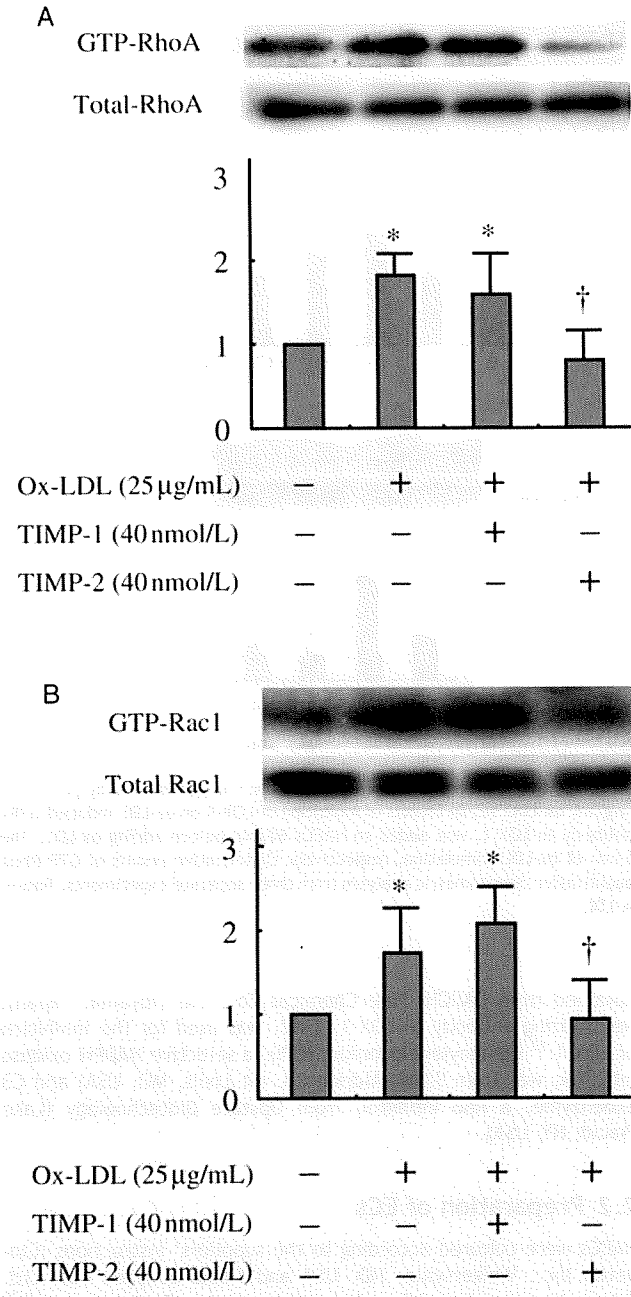

Figure 2 Effects of TIMP-1 and TIMP-2 on ox-LDL-triggered GTP-loading of RhoA (*A*) and Rac1 (*B*). HAECs were pretreated with 40 nmol/L TIMP-1 or TIMP-2 for 60 min before adding ox-LDL. After 5 and 15 min of ox-LDL stimulation, the GTP-loading of RhoA and Rac1 was determined. TIMP indicates tissue inhibitor of metalloproteinase. Bars are mean ± SD of quantitative densitometric analyses from three separate experiments. Representative immunoblots are shown at the top. $^{*}P < 0.05$ vs. control; $^{\dagger}P < 0.05$ vs. ox-LDL.

an Amersham ECL system (Amersham Pharmacia Biotech UK Ltd, Buckinghamshire, UK).

2.5 GTP/GDP exchange of RhoA and Rac1

GTP-bound active forms of RhoA and Rac1 were determined by pull-down assay as described previously.[4,20,22] Extracts of HAECs were incubated at 4°C for 45 min with glutathione-Sepharose 4B beads coupled with glutathione-S-transferase (GST)-rhotekin fusion protein for determination of RhoA activity or GST-p21-activated

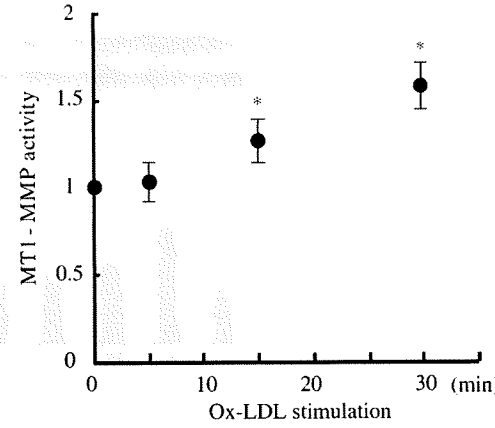

Figure 3 Plasma membrane fractions were extracted from HAECs at the time indicated after ox-LDL stimulation, and thereafter the activity of MT1-MMP was determined as described in the Methods section. Results are expressed as mean ± SD of three separate experiments performed in pentaplicate. $^{*}P < 0.05$ vs. control.

kinase for determination of Rac1 activity. Bound RhoA and Rac1 were semi-quantitatively detected by western blotting.

2.6 Measurement of MT1-MMP activity of membrane fractions

To evaluate MT1-MMP activity, we prepared membrane fractions of HAECs as described previously.[4,21] Briefly, cells were lysed with a hypotonic buffer, then sonicated and centrifuged at 15 000 *g* for 10 min. The separated membrane fractions were assessed by the commercially available fluorescent assay kit (SensoLyte 520 MMP-14 assay kit, AnaSpec, San Jose, CA, USA) according to the manufacturer's instructions.

2.7 Small interfering RNA

MT1-MMP expression was silenced by siRNA 5′-CUGGCAGUUCGGC UAGAUUUC-3′ (sense strand for MT1-MMP) (RNAi Co., Ltd, Tokyo, Japan).[23] HAECs were transfected with double-strand siRNA in serum-free medium mixed with oligofectamine (Invitrogen, Carlsbad, CA, USA) according to the manufacturer's instructions. Four hours after transfection, HAECs were incubated in a medium containing 2% foetal bovine serum (FBS) for 48 h. Alternatively, cells were treated with an irrelevant siRNA 5′-GUACCGCACGUCA UUCGCAUC-3′ (sense strand) as a negative control.

2.8 Generation of anti-human LOX-1 monoclonal antibodies

Anti-human LOX-1 monoclonal antibodies were generated by immunizing Balb/c mice subcutaneously with the recombinant protein of the extracellular domain of LOX-1, LOX-1(61–273).[24] The splenocytes from the immunized mice were fused with myeloma cell line, P3U1, and the resultant hybridomas were screened using enzyme-linked immunosorbent assay to the antigen. Among the positive clones, purified monoclonal antibody from clone #1-1 was used for western blotting, and another antibody from #10-1 was used for immunocytochemistry.

2.9 Fluorescent immunostaining

A mouse monoclonal antibody available to LOX-1 (termed #10-1) was used for immunostaining.[8] HAECs cultured on chamber slides were fixed in 10% formalin for 10 min, and then incubated with the antibodies to LOX-1 and MT1-MMP (Chemicon International, Inc., Temecula, CA, USA) at room temperature for 60 min. After washing, anti-mouse Alexa 488 and anti-rabbit Alexa 594 (Molecular

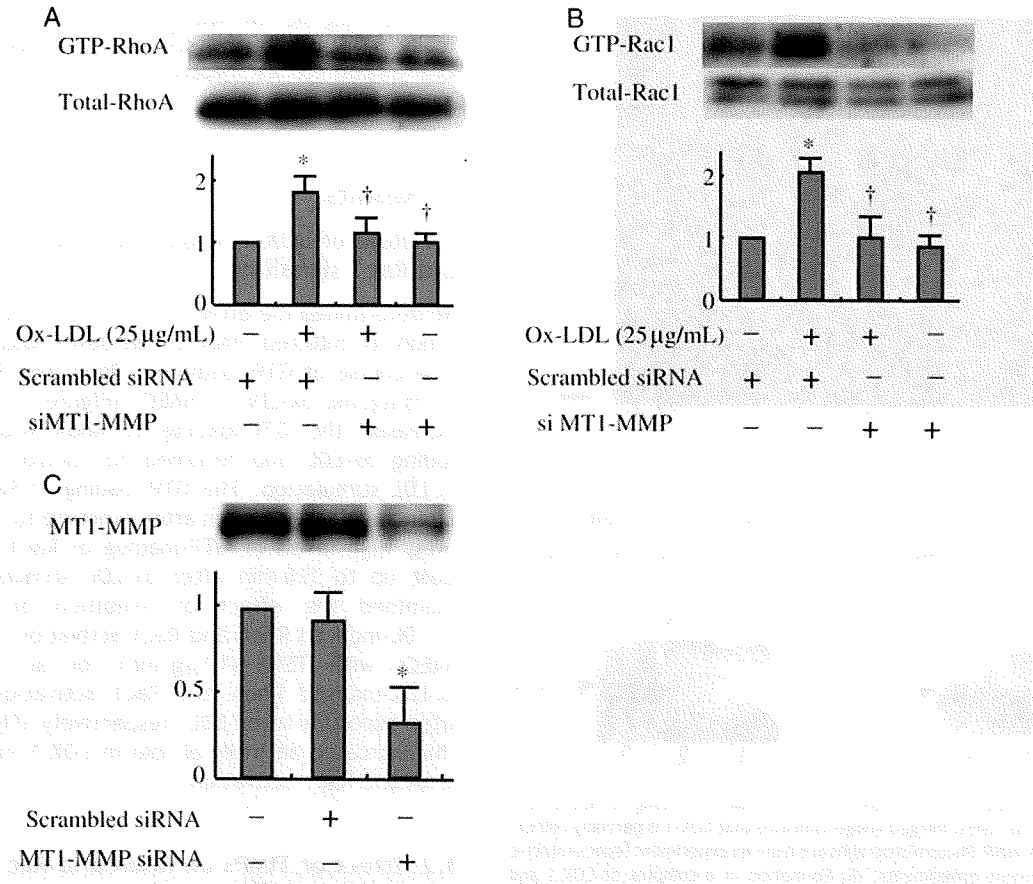

Figure 4 Role of MT1-MMP in ox-LDL-triggered RhoA and Rac1 activation. (*A*, *B*) Effect of knockdown of MT1-MMP by siRNA on increased GTP-loading of RhoA and Rac1 caused by ox-LDL. Cells were incubated in the presence of 25 μg/mL ox-LDL after transfection of MT1-MMP siRNA or scrambled siRNA. The amounts of the GTP-bound forms of RhoA and Rac1 were determined by western blotting. Bars are mean ± SD of four separate experiments. Representative immunoblots from four separate experiments are shown. $^{*}P < 0.05$ vs. control; $^{\dagger}P < 0.05$ vs. ox-LDL. (*C*) Effect of knockdown of MT1-MMP by siRNA on the MT1-MMP protein level as determined by western blotting. Bars are mean ± SD of three separate experiments. Representative immunoblots from three independent experiments are shown. $^{*}P < 0.05$ vs. control.

Probes, Eugene, OR, USA) were reacted for 60 min. Stained cells were stored in the dark until they were analyzed by a confocal microscope (Olympus, Tokyo, Japan).

2.10 Immunoprecipitation

HAECs were extracted in a RIPA buffer (Sigma–Aldrich), and the lysates were centrifuged at 10 000 *g* at 4°C. The supernatant was precleared and reacted with anti-MT1-MMP (Chemicon) and anti-LOX-1 antibody (R&D Systems Inc., Minneapolis, MN, USA) at a concentration of 1.0 μg/mL, respectively. Immunoprecipitated protein was resolved by sodium dodecyl sulfate–polyacrylamide gel electrophoresis, followed by western blotting of LOX-1 and MT1-MMP, respectively. The positive controls of endothelial cell lysate were loaded. We used the primary antibody against LOX-1 (termed #1-1) and MT1-MMP (Chemicon), and anti-mouse or anti-rabbit IgG True blot™ (eBioscience, Inc., San Diego, CA, USA), which detects native antibody but not the denatured 55 kDa heavy chain and 23 kDa light chains of the immunoprecipitating antibody, as the secondary antibody.

2.11 Adenovirus gene transfer

HAECs were infected with adenoviruses encoding a dominant negative form of N19RhoA, N17Rac or *LacZ* at a multiplicity of infection of approximately 50 as described previously.[22,25] This procedure resulted in the expression of *LacZ* as a marker gene in nearly 100% of the transfected cells. After transfection, cells were washed three times with PBS and incubated for 48 h in medium containing 2% FBS, followed by the experiments.

2.12 EC invasion assay

EC invasion was assayed by a commercially available kit (BD Biocoat™ Angiogenesis System: Endothelial Cell Invasion, BD Biosciences, Bedford, MA, USA) according to the manufacturer's instructions. Briefly, HAECs were pretreated with N19RhoA or MT1-MMP siRNA as described above and then stimulated with 25 μg/mL ox-LDL for 12 h. Invasive cells were fluorescently labelled with Calcein-AM and the fluorescence intensity was quantitatively determined by Image J 1.34 (National Institutes of Health, Bethesda, MD, USA).

2.13 Measurement of intracellular ROS generation

Detection of intracellular ROS generation was performed by a previously established method using the ROS-sensitive fluorescent probe 2′,7′-dichlorodihydro-fluorescein-diacetate (H_2DCF-DA) (Molecular Probes).[5] HAECs were incubated in 2% FBS-containing medium and 10 μmol/L H_2DCF-DA for 10 min. Ox-LDL (25 μg/mL) was added to the cells and incubated for up to 60 min at 37°C. The fluorescence was measured using a fluorescent microscope (Olympus) at an excitation and emission wavelength of 475 nm and 525 nm, respectively. DCF fluorescence intensity was quantitatively determined by Image J 1.34. For each photograph, the cellular and background fluorescence values were obtained by tracing the

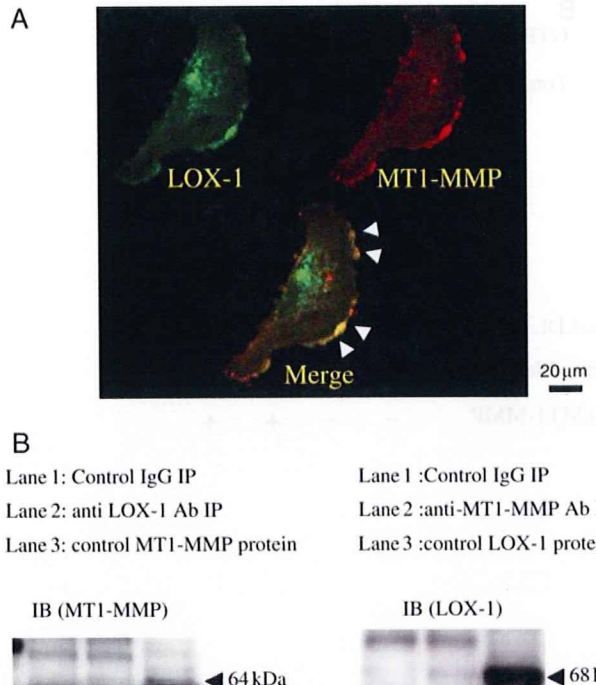

Figure 5 (*A*) Association of LOX-1 and MT1-MMP according to fluorescent immunohistochemistry. Merged image indicates that LOX-1 is partially colocalized with MT1-MMP. Photomicrographs are from an experiment representative of 10 independent experiments. (*B*) Formation of a complex of LOX-1 and MT1-MMP as determined by immunoprecipitation. In the left panel, 64 kDa band recognized by immunoblotting with anti-MT1-MMP antibody was detected in the LOX-1-immunoprecipitates (lane 2). Immunoprecipitates made using an isotype-matched control antibody did not show 64-kDa band (left panel, lane 1), whereas 64 kDa band was recognized in control cell lysate. In a reversed experiment, LOX-1 (70 kDa) was detected from MT1-MMP immunoprecipitates (right panel, lane 2), whereas control antibody-associated immunoprecipitates did not contain the LOX-1 band (right panel, lane 1). Each control immunoblot of endothelial cell lysate is shown in lane 3.

shape of cells. Results were displayed in a ratiometric fashion normalized for the control condition.

2.14 Measurement of NADPH oxidase activity

Since ox-LDL increases NADPH oxidase activity, the enzymatic activities of NADPH oxidase of homogenates of the cells were assessed by lucigenin-enhanced chemiluminescence (L-CL) as previously described.[26] The assay solution contained 50 mmol/L HEPES (pH 7.4), 1.0 mmol/L EDTA, 6.5 mmol/L $MgCl_2$, 5.0 μmol/L lucigenin as an electron acceptor and 1 mmol/L NADPH as a substrate. After preincubation at 37°C for 10 min, the reaction was started by adding 50 μg of homogenate. Final volume of the reaction solution was 1.0 mL. Photon emission was continuously recorded for 15 min with a CL reader (ALOKA, BLR-201, Tokyo, Japan). The chemiluminescent signals observed in the absence of homogenates were subtracted from the chemiluminescence signals of the samples. The chemiluminescence signal was corrected for the protein concentration of each cell homogenate and expressed as counts per minute (cpm) per milligram protein for a 15-min period. In some experiments, the homogenates were preincubated with 10 μmol/L DPI for 20 min before L-CL measurement.

2.15 Densitometric analysis and statistical analyses

After scanning blots into a computer (EPSON GT5500ART, Tokyo, Japan), the optical densities of individual immunoblots were analyzed using the NIH IMAGE Program software as described previously.[18,20] Statistical analyses were performed using ANOVA with Scheffé's *post hoc* test if appropriate. A value of $P < 0.05$ was considered significant.

3. Results

3.1 Role of LOX-1 in ox-LDL-induced RhoA and Rac1 signalling

We determined the effect of ox-LDL on RhoA and Rac1 activation in cultured HAECs. Pull-down assays revealed the time-course of GTP-loading of RhoA and Rac1 in response to 25 μg/mL ox-LDL in HAECs (*Figure 1A* and *B*). Ox-LDL increased the GTP-loading of RhoA within 5 min after adding ox-LDL and returned to control after 15 min of ox-LDL stimulation. The GTP-loading of Rac1 was induced 5 min and peaked 15 min after exposure to ox-LDL. The relatively high levels of GTP-loading of Rac1 persisted for at least up to 120 min after ox-LDL stimulation. Next, we examined the effect of inhibition of LOX-1 on the ox-LDL-induced RhoA and Rac1 activation. Pretreatment of HAECs with TS92 (10 μg/mL) for an hour prevented ox-LDL-induced RhoA and Rac1 activation 5 and 15 min after exposure to ox-LDL, respectively (*Figure 1C* and *D*). This indicated an integral role of LOX-1 in ox-LDL-induced RhoA and Rac1 activation.

3.2 Effect of TIMPs on RhoA and Rac1 activation induced by ox-LDL

To clarify the relation between secreted MMPs or MT-MMPs and LOX-1-mediated RhoA and Rac1 activation, HAECs were pretreated with 40 nmol/L TIMP-1 and TIMP-2 for 60 min before adding ox-LDL. *Figure 2A* and *B* show that TIMP-2, but not TIMP-1, inhibited the GTP-loading of RhoA and Rac1 caused by ox-LDL. TIMP-1 or TIMP-2 alone did not alter the basal levels of RhoA and Rac1 in untreated HAECs (data not shown). These findings suggest that MT-MMPs are upstream of ox-LDL-triggered RhoA and Rac1 activation.

3.3 MT1-MMP activity

Since MT1-MMP is one of the well-characterized MT-MMPs, we first measured the activity of MT1-MMP in response to ox-LDL stimulation within 30 min. Ox-LDL induced a significant increase in the activity of MT1-MMP after 15 and 30 min of stimulation (*Figure 3*).

3.4 Role of MT1-MMP in ox-LDL-induced RhoA and Rac1 signalling

Then, we examined the role of MT1-MMP in ox-LDL-induced RhoA and Rac1 activation through LOX-1. HAECs were transfected with siRNA to MT1-MMP before exposure to ox-LDL. In the transfected cells, knockdown of MT1-MMP prevented the ox-LDL-triggered activation of RhoA and Rac1 as determined by pull-down assays (*Figure 4A* and *B*). *Figure 4C* shows the effect of the transfection of MT1-MMP siRNA on the MT1-MMP protein level as determined by western blotting, indicating the approximately 70% reduction in the MT1-MMP level by treatment with the siRNA.

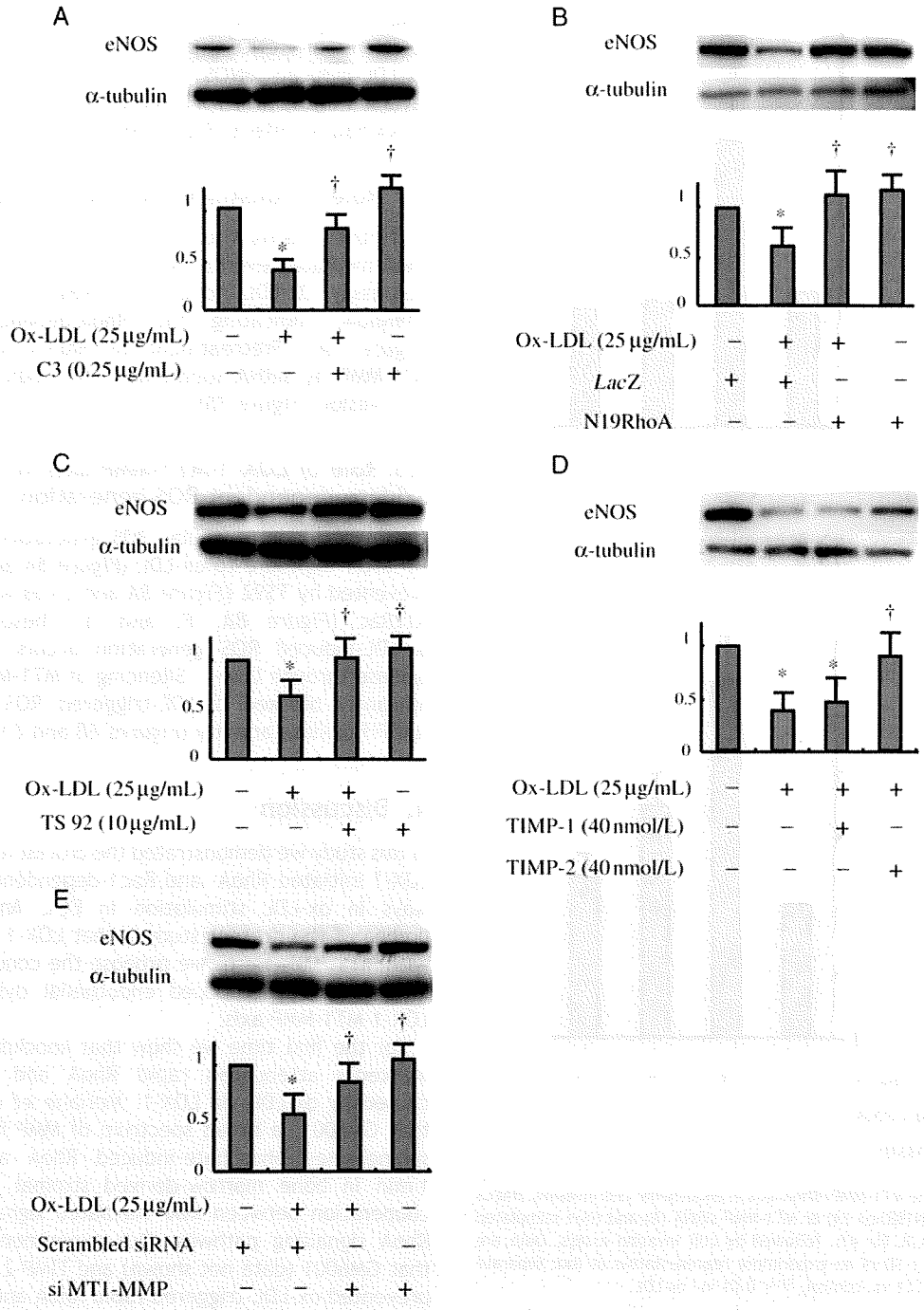

Figure 6 Role of the LOX-1/MT1-MMP axis in RhoA-dependent eNOS protein expression. (*A*, *B*) Effect of inhibition of RhoA by C3 exoenzyme and N19RhoA on ox-LDL-induced eNOS downregulation. HAECs were treated with 0.25 μg/mL of C3 exoenzyme overnight or infected with adenoviruses encoding N19RhoA or *LacZ* and then stimulated with 25 μg/mL ox-LDL for 18 h, followed by western blotting. (*C*) Effect of inhibition of LOX-1 on ox-LDL-induced eNOS downregulation. Cells were treated with 10 μg/mL TS92 for 1 h and then stimulated with 25 μg/mL ox-LDL for 18 h, followed by western blotting. (*D*, *E*) Effects of TIMP-2 and knockdown of MT1-MMP on ox-LDL-induced eNOS downregulation. Immunoblots are from an experiment representative of four similar experiments. Quantitative results of eNOS expression were normalized by α-tubulin levels. Bars are mean ± SD of quantitative densitometric analyses from three separate experiments. $^{*}P < 0.05$ vs. control; $^{\dagger}P < 0.05$ vs. ox-LDL.

3.5 Molecular interaction of LOX-1 and MT1-MMP

To determine the distribution of LOX-1 and MT1-MMP in cultured HAECs, we performed immunostaining. *Figure 5A* shows the expression of LOX-1 and MT1-MMP, as well as the merged image, respectively, indicating that LOX-1 was partially colocalized with MT1-MMP in HAECs.

To clarify the interaction of LOX-1 with MT1-MMP, we first performed the immunoprecipitation using an initial antibody to LOX-1. Although little or no expression was detected by normal mouse IgG as a negative control antibody (*Figure 5B*, left panel, lane 1), the band of 64 kDa of MT1-MMP was detected in the LOX-1-associated immunoprecipitates (*Figure 5B*, left panel, lane 2). Counter experiment using anti-MT1-MMP antibody revealed that the band of LOX-1 (Mr 70 kDa) was recognized in the MT1-MMP-immunoprecipitates (*Figure 5B*, right panel, lane 2). These

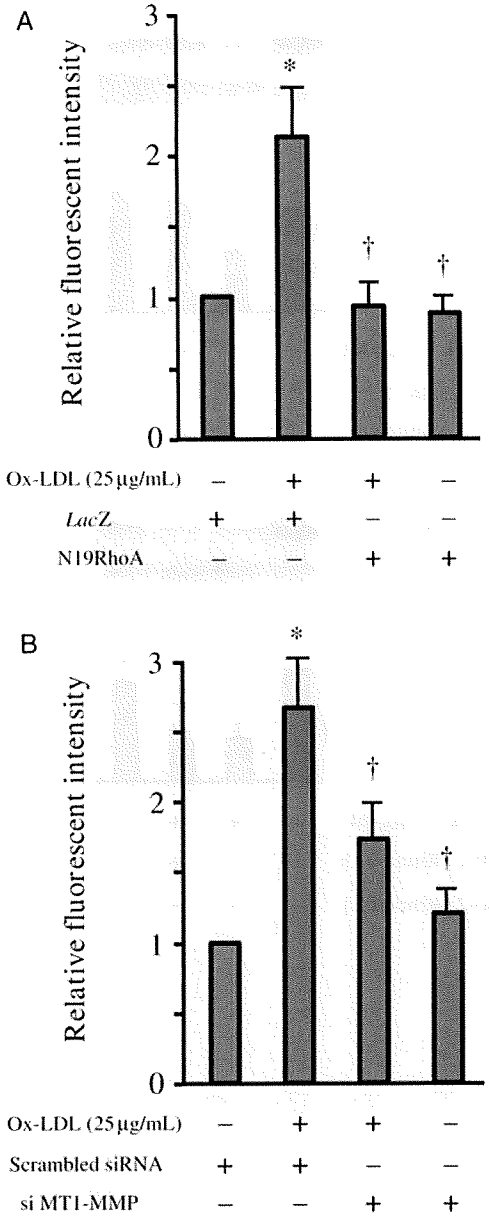

Figure 7 Role of the MT1-MMP/RhoA axis in endothelial cell invasion. HAECs were treated with N19RhoA (*A*) or MT1-MMP siRNA (*B*) and then stimulated with 25 μg/mL ox-LDL for 4 h, followed by cell invasion assays. Data are expressed as mean ± SD of an experiment representative of four separate experiments. $^{*}P < 0.01$ vs. control; $^{\dagger}P < 0.01$ vs. ox-LDL.

results strongly suggested that LOX-1 forms a complex with MT1-MMP. Exposure to ox-LDL did not change the level of formation of LOX-1 and MT1-MMP (data not shown).

3.6 Role of MT1-MMP-RhoA axis in ox-LDL-induced downregulation of eNOS protein expression

First, we confirmed that ox-LDL-induced downregulation of eNOS protein expression is mediated via RhoA activation in our culture system. Inhibition of RhoA by C3 exoenzyme (*Figure 6A*) and dominant-negative RhoA (*Figure 6B*) reversed ox-LDL-induced decrease of eNOS protein expression. Treatment of HAECs with TS92 for LOX-1 inhibition reversed the ox-LDL-induced eNOS protein downregulation after 18 h of incubation (*Figure 6C*). In addition, TIMP-2, but not TIMP-1, prevented ox-LDL-induced downregulation of eNOS protein expression (*Figure 6D*). Ox-LDL-induced eNOS protein downregulation was also reversed in the MT1-MMP-silenced cells, whereas scrambled siRNA had no effect (*Figure 6E*).

3.7 Role of RhoA-MT1-MMP axis in cell invasion

To further clarify the role of the MT1-MMP/RhoA axis in RhoA-mediated events, we performed an endothelial invasion assay. Ox-LDL-induced EC invasion was attenuated by N19RhoA, indicating the RhoA-dependent mechanism (*Figure 7A*). Pretreatment of HAECs with silencing of MT1-MMP by siRNA suppressed the oxidized LDL-triggered EC invasion (*Figure 7B*).

3.8 Role of LOX-1-MT1-MMP axis in NADPH oxidase-dependent ROS generation

The levels of intracellular ROS generation were increased 1 h after exposure to ox-LDL (*Figure 8A* and *B*), which was prevented by TS92 (*Figure 8A* and *C*) as well as by DPI and N17Rac (*Figure 8A, E,* and *I*). These indicated that ox-LDL-induced ROS generation occurs via Rac1/NADPH oxidase through LOX-1. Silencing of MT1-MMP by siRNA significantly blocked ox-LDL-triggered ROS generation and NADPH oxidase activity (*Figures 8B* and *C*).

4. Discussion

In this study we demonstrated the crucial role of MT1-MMP in LOX-1-initiated RhoA- and Rac1-dependent signalling pathways in ox-LDL stimulation in ECs. Another important finding of the present study is that LOX-1 forms a complex with MT1-MMP. Here, we propose the concept of the regulation of ox-LDL-induced endothelial dysfunction by the LOX-1-MT1-MMP axis.

For the first time we show that knockdown of MT1-MMP markedly attenuated rapid RhoA and Rac1 activation caused by ox-LDL via LOX-1. Meriane *et al.*[27] have shown that GM6001, a broad spectrum of MMP inhibitor, blocked sphingosine-1-phosphate-induced RhoA activation within 1 min in bone marrow-derived stromal cells, suggesting cooperation between MMP-mediated signalling events and RhoA signalling pathway. Our experiments demonstrated that GM6001 (data not shown) and TIMP-2, but not TIMP-1, prevented ox-LDL-triggered rapid RhoA and Rac1 activation in HAECs, suggesting that extracellular domain of MT1-MMP may play a role in the signal transduction of ox-LDL-exposed cells via LOX-1. In fact, the increase in MT1-MMP activity was induced by ox-LDL within 15 min. However, the detailed mechanism(s) remain(s) to be clarified.

The present study indicates that MT1-MMP is upstream of ox-LDL-stimulated RhoA and Rac1 activation. It is generally accepted that MT1-MMP is an MMP-2 activator.[13,28,29] This raises the issue whether or not inhibition of MMP-2 might prevent ox-LDL-triggered RhoA and Rac1 activation in our experimental system. We found that TIMP-1, which inhibits MMP-2 but not MT-MMPs, did not suppress the ox-LDL-dependent RhoA and Rac1 activation. These results suggest that MMP-2 is not involved in ox-LDL-triggered RhoA and Rac1 signalling pathways in ECs.

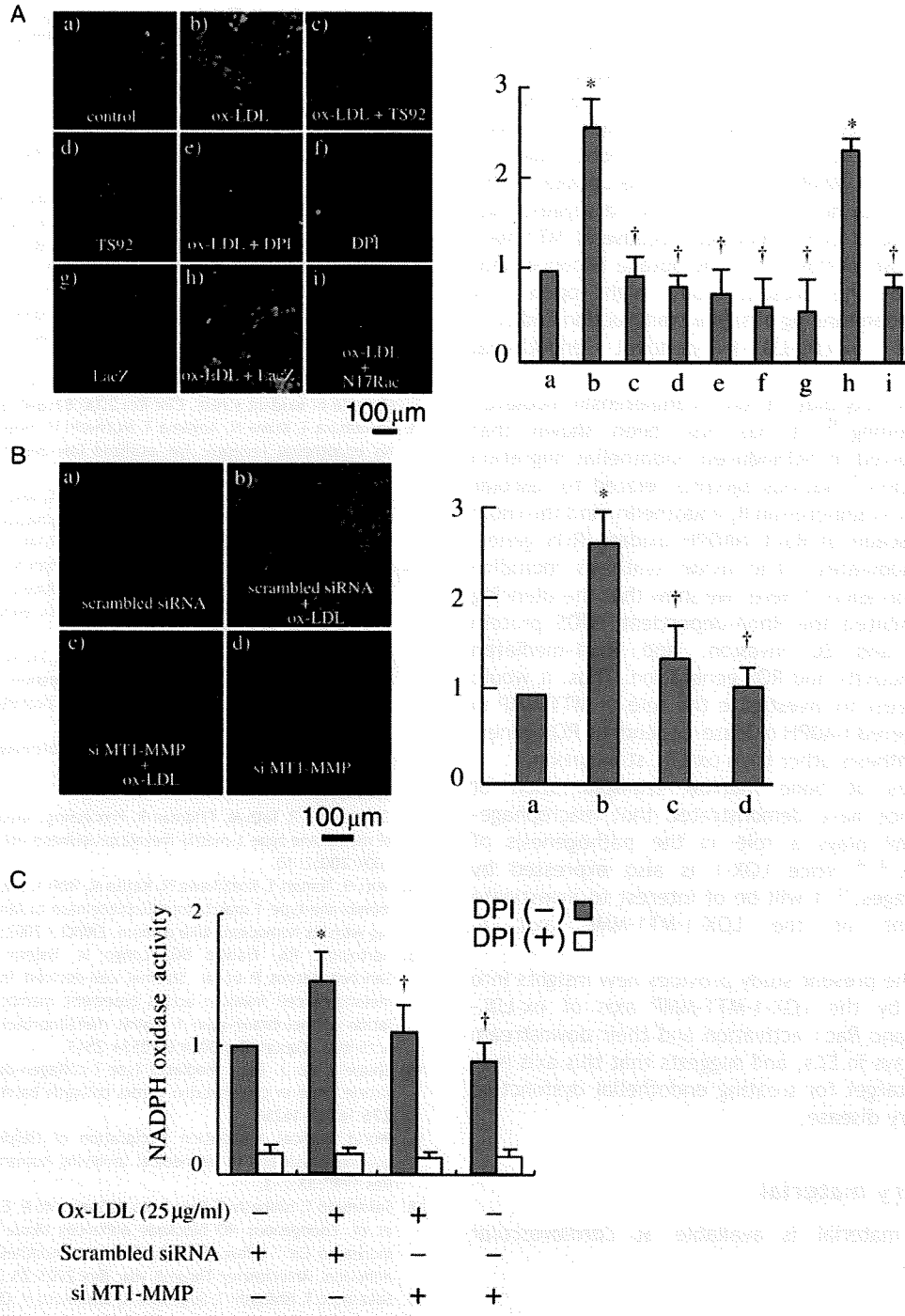

Figure 8 (*A*) HAECs were stimulated with 25 μg/mL ox-LDL for 60 min with or without pretreatment using 10 μg/mL TS92 for 1 h or 10 μmol/L DPI for 30 min. Cells were also infected with adenoviruses encoding N17Rac or *Lac*Z (g, h, i). Then, intracellular ROS formation was assessed by H2DCF-DA oxidation-based fluorescence. Photomicrographs are from an experiment representative of six independent experiments. Bars represent mean ± SD of six independent experiments. (*B*, *C*) Effect of inhibition of MT1-MMP on ox-LDL-induced ROS generation and NADPH oxidase activity. (*B*) HAECs were stimulated with 25 μg/mL ox-LDL for 60 min with MT1-MMP siRNA or scrambled siRNA. Intracellular ROS formation was then assessed by H2DCF-DA oxidation-based fluorescence. Photomicrographs are from an experiment representative of six independent experiments. Bars are mean ± SD of quantitative analyses from six separate experiments. (*C*) Endothelial NADPH oxidase activity was measured with or without silencing of MT1-MMP 15 min after adding ox-LDL. Treatment of endothelial homogenates with DPI abolished the enzymatic activity of NAPDH oxidase. Data are the mean ± SD from five separate experiments. $^{*}P < 0.01$ vs. control; $^{\dagger}P < 0.01$ vs. ox-LDL.

Fluorescent immunostaining revealed that LOX-1 was colocalized with MT1-MMP to some degree in cultured HAECs. The notable finding of the present study by immunoprecipitation is that LOX-1 formed a complex with MT1-MMP in HAECs. To the best of our knowledge, the present study is the first to show the formation of a complex of LOX-1 with another molecule in ECs. It would be of importance to determine whether LOX-1 and MT1-MMP forms a complex *in vivo*. Our experiments suggested that LOX-1 also formed a complex with MT1-MMP in the aortae of Watanabe heritable hyperlipidaemic rabbits (data not shown). The issue should be extensively investigated in terms of the physiopathology

of vascular remodelling. We also found that ox-LDL did not change the levels of a complex of LOX-1 and MT1-MMP, although ox-LDL increased the protein expression of LOX-1 and MT1-MMP after 18 h of incubation (data not shown). We further attempted to determine whether MT1-MMP modulates LOX-1 in cultured HAECs. Our data indicated that silencing of MT1-MMP did not alter the uptake of DiI-labelled ox-LDL (data not shown). This would suggest that there is no change in LOX-1 function because of MT1-MMP knockdown at least inasfar as ox-LDL uptake is concerned. These findings of the present study might open new avenues in the understanding of signal transduction and physiopathology of ox-LDL-LOX-1-dependent endothelial dysfunction.

MT1-MMP reportedly plays a role in angiotensin-mediated vascular remodelling.[30] It has also been shown that MT1-MMP is involved in NO-induced endothelial migration and tube formation.[31] Various agonists related to vascular remodelling such as angiotensin II, endothelin, and thrombin regulate the cascade of Rac1/NADPH oxidase/ROS generation, which modulates nitric oxide synthesis including eNOS protein expression.[32] Here, we show that the silencing of MT1-MMP inhibited the RhoA-dependent eNOS protein downregulation and EC invasion, and Rac1-mediated NADPH oxidase activity and ROS generation. Thus, it would be of great interest to investigate the role of MT1-MMP in the agonist-triggered NADPH oxidase-dependent ROS generation and NO synthesis other than ox-LDL stimulation.

Recent studies of bone marrow transplantation of MT1-MMP$^{-/-}$ mice have demonstrated that macrophage-derived MT1-MMP plays a role in the pathogenesis of plaque stability.[33,34] Since LOX-1 is also expressed by plaque macrophages,[35] it will be of interest to investigate the involvement of the LOX-1-MT1-MMP axis in macrophages.

In summary, the present study provides new insights into the regulation by the LOX-1-MT1-MMP axis of ox-LDL-mediated RhoA and Rac1 activation and their downstream signalling pathways in ECs, and suggests that this axis may be a promising target for treating endothelial dysfunction in coronary artery disease.

Supplementary material

Supplementary material is available at *Cardiovascular Research* online.

Funding

This work was supported in part by Grants-in-Aid for Scientific Research from the Japan Society for the Promotion of Science (14370232, 1979056, and 20790538), Fukushima Medical University Research Project, Takeda Science Foundation, and The Uehara Memorial Foundation.

Conflict of interest: none declared.

References

1. Ross R. The pathogenesis of atherosclerosis: a perspective for the 1990s. *Nature* 1993;**362**:801–809.
2. Stocker R, Keaney JF Jr. Role of oxidative modifications in atherosclerosis. *Physiol Rev* 2004;**84**:1381–1478.
3. Laufs U, La Fata V, Plutzky J, Liao JK. Upregulation of endothelial nitric oxide synthase by HMG CoA reductase inhibitors. *Circulation* 1998;**97**:1129–1135.
4. Yokoyama K, Ishibashi T, Ohkawara H, Kimura J, Matsuoka I, Sakamoto T *et al.* HMG-CoA reductase inhibitors suppress intracellular calcium mobilization and membrane current induced by lysophosphatidylcholine in endothelial cells. *Circulation* 2002;**105**:962–967.
5. Cominacini L, Pasini AF, Garbin U, Davoli A, Tosetti ML, Campagnola M *et al.* Oxidized low density lipoprotein (ox-LDL) binding to ox-LDL receptor-1 in endothelial cells induces the activation of NF-kappaB through an increased production of intracellular reactive oxygen species. *J Biol Chem* 2000;**275**:12633–12638.
6. Gregg D, Rauscher FM, Goldschmidt-Clermont PJ. Rac regulates cardiovascular superoxide through diverse molecular interactions: more than a binary GTP switch. *Am J Physiol Cell Physiol* 2003;**285**:C723–C734.
7. Cai H, Harrison DG. Endothelial dysfunction in cardiovascular diseases: the role of oxidant stress. *Circ Res* 2000;**87**:840–844.
8. Sawamura T, Kume N, Aoyama T, Moriwaki H, Hoshikawa H, Aiba Y *et al.* An endothelial receptor for oxidized low-density lipoprotein. *Nature* 1997;**386**:73–77.
9. Szmitko PE, Wang CH, Weisel RD, Jeffries GA, Anderson TJ, Verma S. Biomarkers of vascular disease linking inflammation to endothelial activation: Part II. *Circulation* 2003;**108**:2041–2048.
10. Li D, Liu L, Chen H, Sawamura T, Ranganathan S, Mehta JL. LOX-1 mediates oxidized low-density lipoprotein-induced expression of matrix metalloproteinases in human coronary artery endothelial cells. *Circulation* 2003;**107**:612–617.
11. Rajavashisth TB, Xu XP, Jovinge S, Meisel S, Xu XO, Chai NN *et al.* Membrane type 1 matrix metalloproteinase expression in human atherosclerotic plaques: evidence for activation by proinflammatory mediators. *Circulation* 1999;**99**:3103–3109.
12. Baker AH, Edwards DR, Murphy G. Metalloproteinase inhibitors: biological actions and therapeutic opportunities. *J Cell Sci* 2002;**115**:3719–3727.
13. Osenkowski P, Toth M, Fridman R. Processing, shedding, and endocytosis of membrane type 1-matrix metalloproteinase (MT1-MMP). *J Cell Physiol* 2004;**200**:2–10.
14. Mori H, Tomari T, Koshikawa N, Kajita M, Itoh Y, Sato H *et al.* CD44 directs membrane-type 1 matrix metalloproteinase to lamellipodia by associating with its hemopexin-like domain. *EMBO J* 2002;**21**:3949–3959.
15. Bartolome RA, Galvez BG, Longo N, Baleux F, Van Muijen GN, Sanchez-Mateos P *et al.* Stromal cell-derived factor-1alpha promotes melanoma cell invasion across basement membranes involving stimulation of membrane-type 1 matrix metalloproteinase and Rho GTPase activities. *Cancer Res* 2004;**64**:2534–2543.
16. Zhuge Y, Xu J. Rac1 mediates type I collagen-dependent MMP-2 activation. Role in cell invasion across collagen barrier. *J Biol Chem* 2001;**276**:16248–16256.
17. World Medical Association Declaration of Helsinki. Recommendation guiding physicians in biomedical involving human subjects. *Cardiovasc Res* 1997;**35**:2–3.
18. Sakamoto T, Ishibashi T, Sakamoto N, Sugimoto K, Egashira K, Ohkawara H *et al.* Endogenous NO blockade enhances tissue factor expression via increased Ca^{2+} influx through MCP-1 in endothelial cells by monocyte adhesion. *Arterioscler Thromb Vasc Biol* 2005;**25**:2005–2011.
19. Sakamoto T, Ishibashi T, Sugimoto K, Sakamoto N, Ohkawara H, Niinuma M *et al.* RhoA-dependent PAI-1 gene expression induced in endothelial cells by monocyte adhesion mediates geranylgeranyl transferase I and Ca^{2+} signaling. *Atherosclerosis* 2007;**193**:44–54.
20. Ohkawara H, Ishibashi T, Sakamoto T, Sugimoto K, Nagata K, Yokoyama K *et al.* Thrombin-induced rapid geranylgeranylation of RhoA as an essential process for RhoA activation in endothelial cells. *J Biol Chem* 2005;**280**:10182–10188.
21. Yokoyama K, Ishibashi T, Yi-qiang L, Nagayoshi A, Teramoto T, Maruyama Y. Interleukin-1beta and interleukin-6 increase levels of apolipoprotein B mRNA and decrease accumulation of its protein in culture medium of HepG2 cells. *J Lipid Res* 1998;**39**:103–113.
22. Ishibashi T, Sakamoto T, Ohkawara H, Nagata K, Sugimoto K, Sakurada S *et al.* Integral role of RhoA activation in monocyte adhesion-triggered tissue factor expression in endothelial cells. *Arterioscler Thromb Vasc Biol* 2003;**23**:681–687.
23. Naito Y, Yamada T, Ui-Tei K, Morishita S, Saigo K. siDirect: highly effective, target-specific siRNA design software for mammalian RNA interference. *Nucleic Acids Res* 2004;**32**:W124–W129. (Web Server issue).

24. Fujita Y, Kakino A, Nishimichi N, Yamaguchi S, Sato Y, Machida S *et al.* Oxidized LDL receptor LOX-1 binds to C-reactive protein and mediates its vascular effects. *Clin Chem* 2009;**55**:285–294.
25. Ryu Y, Takuwa N, Sugimoto N, Sakurada S, Usui S, Okamoto H *et al.* Sphingosine-1-phosphate, a platelet-derived lysophospholipid mediator, negatively regulates cellular Rac activity and cell migration in vascular smooth muscle cells. *Circ Res* 2002;**90**:325–332.
26. Ejiri J, Inoue N, Kobayashi S, Shiraki R, Otsui K, Honjo T *et al.* Possible role of brain-derived neurotrophic factor in the pathogenesis of coronary artery disease. *Circulation* 2005;**112**:2114–2120.
27. Meriane M, Duhamel S, Lejeune L, Galipeau J, Annabi B. Cooperation of matrix metalloproteinases with the RhoA/Rho kinase and mitogen-activated protein kinase kinase-1/extracellular signal-regulated kinase signaling pathways is required for the sphingosine-1-phosphate-induced mobilization of marrow-derived stromal cells. *Stem Cells* 2006;**24**:2557–2565.
28. Stawowy P, Meyborg H, Stibenz D, Borges Pereira Stawowy N, Roser M, Thanabalasingam U *et al.* Furin-like proprotein convertases are central regulators of the membrane type matrix metalloproteinase-pro-matrix metalloproteinase-2 proteolytic cascade in atherosclerosis. *Circulation* 2005;**111**:2820–2827.
29. El Bedoui J, Oak MH, Anglard P, Schini-Kerth VB. Catechins prevent vascular smooth muscle cell invasion by inhibiting MT1-MMP activity and MMP-2 expression. *Cardiovasc Res* 2005;**67**:317–325.
30. Jesmin S, Sakuma I, Hattori Y, Kitabatake A. Role of angiotensin II in altered expression of molecules responsible for coronary matrix remodeling in insulin-resistant diabetic rats. *Arterioscler Thromb Vasc Biol* 2003; **23**:2021–2026.
31. Genís L, Gonzalo P, Tutor AS, Gálvez BG, Martínez-Ruiz A, Zaragoza C *et al.* Functional interplay between endothelial nitric oxide synthase and membrane type 1 matrix metalloproteinase in migrating endothelial cells. *Blood* 2007;**110**:2916–2923.
32. Cai H. Hydrogen peroxide regulation of endothelial function: origins, mechanisms, and consequences. *Cardiovasc Res* 2005;**68**: 26–36.
33. Schneider F, Sukhova GK, Aikawa M, Canner J, Gerdes N, Tang SM *et al.* Matrix-metalloproteinase-14 deficiency in bone-marrow-derived cells promotes collagen accumulation in mouse atherosclerotic plaques. *Circulation* 2008;**117**:931–939.
34. Xiong W, Knispel R, MacTaggart J, Greiner TC, Weiss SJ, Baxter BT. Membrane-type 1 matrix metalloproteinase regulates macrophage-dependent elastolytic activity and aneurysm formation *in vivo*. *J Biol Chem* 2009;**284**:1765–1771.
35. Kataoka H, Kume N, Miyamoto S, Minami M, Moriwaki H, Murase T *et al.* Expression of lectin-like oxidized low-density lipoprotein receptor-1 in human atherosclerotic lesions. *Circulation* 1999;**99**:3110–3117.

ARTHRITIS & RHEUMATISM
Vol. 60, No. 10, October 2009, pp 3007–3016
DOI 10.1002/art.24816

Induction of Bovine Articular Chondrocyte Senescence With Oxidized Low-Density Lipoprotein Through Lectin-like Oxidized Low-Density Lipoprotein Receptor 1

Satoshi Zushi,[1] Masao Akagi,[1] Hideki Kishimoto,[1] Takeshi Teramura,[1] Tatsuya Sawamura,[2] and Chiaki Hamanishi[1]

Objective. **Findings of recent in vivo and in vitro studies suggest that oxidized low-density lipoprotein (ox-LDL) plays a role in the degeneration of cartilage. The purpose of this study was to determine whether ox-LDL induces chondrocyte senescence through binding to lectin-like ox-LDL receptor 1 (LOX-1).**

Methods. **The effects of ox-LDL on senescence of cultured bovine articular chondrocytes (BACs) were investigated by observing senescence-associated (SA) β-galactosidase (β-gal) activity, cell proliferation activity, and telomerase activity. Telomerase activity was measured after adding LY294002 (a specific inhibitor of phosphatidylinositol 3-kinase [PI3K]) or after adding insulin-like growth factor 1 (IGF-1; an activator of PI3K) plus ox-LDL to the culture medium to elucidate the involvement of the PI3K/Akt pathway. Immunoblot analysis was used to investigate whether ox-LDL affects the phosphorylation of Akt. To ascertain whether these effects were attributable to ox-LDL binding to LOX-1, BACs were preincubated with TS-20, an anti-bovine LOX-1 blocking antibody.**

Results. **The activity of SA β-gal was increased and the incorporation of bromodeoxyuridine into BACs was decreased by ox-LDL in a dose-dependent manner. The telomerase activity of BACs was suppressed by the addition of ox-LDL in a time- and dose-dependent manner. LY294002 suppressed the telomerase activity of BACs, and IGF-1 reversed the ox-LDL–induced suppression of telomerase activity. In addition, ox-LDL rapidly decreased the amount of phosphorylated Akt in BACs. Pretreatment of cultured BACs with TS-20 recovered these effects.**

Conclusion. **These data show that ox-LDL binding to LOX-1 induces stress-induced premature senescence of chondrocytes and results in suppression of telomerase activity by inactivating the PI3K/Akt pathway. Oxidized LDL may play an important role in the pathogenesis of osteoarthritis by inducing chondrocyte senescence.**

Oxidized low-density lipoprotein (ox-LDL) was recently recognized to be one of the most important molecules that cause atherosclerosis (1). A novel receptor for ox-LDL, designated lectin-like ox-LDL receptor 1 (LOX-1), was recently cloned from cultured bovine aortic endothelial cells (2). The uptake of ox-LDL through this receptor, which is expressed on the vascular endothelium, is critically involved in endothelial activation and dysfunction in atherogenesis (3). The involvement of lipid peroxidation in the cartilage degeneration associated with both aging and the pathogenesis of osteoarthritis (OA) has been suggested by in vivo (4,5) and in vitro (6,7) studies. Some epidemiologic studies have suggested that OA and atherosclerosis share a common epidemiologic background in terms of the involvement of lipid peroxidation (8,9).

Interestingly, Nakagawa et al (10) showed the expression of LOX-1 and the presence of ox-LDL in chondrocytes from rats with zymosan-induced arthritis (ZIA); in addition, treatment with anti–LOX-1 blocking antibody was shown to suppress articular cartilage degeneration in ZIA, suggesting that ox-LDL binding to

Supported in part by grants from the Ministry of Education, Culture, Sports, Science, and Technology of Japan.

[1]Satoshi Zushi, MD, Masao Akagi, MD, PhD, Hideki Kishimoto, MD, Takeshi Teramura, PhD, Chiaki Hamanishi, MD, PhD: Kinki University School of Medicine, Osaka-Sayama City, Osaka, Japan; [2]Tatsuya Sawamura, MD, PhD: National Cardiovascular Center Research Institute, Suita City, Osaka, Japan.

Address correspondence and reprint requests to Masao Akagi, MD, PhD, Department of Orthopaedic Surgery, Kinki University School of Medicine, 377-2 Ohno-Higashi, Osaka-Sayama City, Osaka 589-8511, Japan. E-mail: makagi@med.kindai.ac.jp.

Submitted for publication January 21, 2009; accepted in revised form June 15, 2009.

LOX-1 is involved in cartilage degeneration. Their in vitro study using cultured rat articular chondrocytes showed that LOX-1 expression is detectable under basal culture conditions and that ox-LDL reduces rat chondrocyte viability through LOX-1, which induces nonapoptotic cell death (11). We previously demonstrated that ox-LDL binding to LOX-1 in cultured bovine articular chondrocytes (BACs) increases the production of intracellular reactive oxygen species, resulting in the activation of NF-κB and the enhancement of monocyte chemoattractant protein 1 production, suggesting that ox-LDL exerts effects similar to those of interleukin-1β on the degradation of articular cartilage (12,13).

These observations suggest that the ox-LDL/LOX-1 system plays a role in both endothelial and chondrocyte dysfunction. More recently, we and other investigators (14,15) have reported the presence of ox-LDL and LOX-1 expression in articular cartilage from patients with rheumatoid arthritis and OA, respectively. In addition, ox-LDL was shown to penetrate the cartilage matrix and to associate with LOX-1, increasing the production of matrix metalloproteinase 3 by cultured explants of human articular cartilage (14). It was further demonstrated that the presence of ox-LDL and the expression of LOX-1 in chondrocytes correlates with grades of OA degeneration in cartilage (15). Simopoulou et al (16) also showed that ox-LDL is detectable in synovial fluid from OA joints and that LOX-1 messenger RNA (mRNA) and protein are expressed in chondrocytes derived from OA cartilage. This growing evidence suggests that the binding of ox-LDL to LOX-1 may modulate the cartilage degeneration seen in OA patients.

Epidemiologic studies have shown that age is the chief risk factor for atherosclerotic diseases (17) as well as for OA (18,19). Both the endothelial cells in atherosclerotic lesions (20,21) and the chondrocytes in OA cartilage (22,23) show attributes of cell senescence, and cell senescence and aging of the tissue are strongly correlated in both diseases. The purpose of the present study was to investigate whether ox-LDL induces cell senescence of cultured BACs. We first investigated whether ox-LDL affects senescence-associated (SA) β-galactosidase (β-gal) activity and cell proliferative ability. Next, we investigated the effects of ox-LDL on the telomerase activity of cultured BACs and on the phosphatidylinositol 3-kinase (PI3K)/Akt pathway, which may be involved in the regulation of the telomerase activity of chondrocytes. We also used a blocking antibody against LOX-1 to investigate whether ox-LDL–induced cell senescence occurs through the binding to LOX-1.

MATERIALS AND METHODS

Reagents. Nonspecific mouse IgG was purchased from Equitech-Bio (Kerrville, TX). LY294002 and recombinant human insulin-like growth factor (IGF-1) were purchased from Sigma (St. Louis, MO). Anti-Akt rabbit IgG, anti–phosphorylated-Akt (anti-pAkt; Ser^{473}) rabbit IgG, and anti-rabbit IgG horseradish peroxidase–linked antibodies were purchased from Cell Signaling Technology (Beverly, MA). The methods we used to prepare the native LDL and ox-LDL have been described previously (2,11).

Primary culture of BACs. Chondrocytes were isolated from articular cartilage of 10-month-old cows by enzymatic digestion with 2 mg/ml of collagenase (Wako Pure Chemical Industries, Osaka, Japan) for 12 hours at 37°C. After filtration, cells were seeded in culture plates and cultured in Dulbecco's modified Eagle's medium (Gibco, Grand Island, NY) supplemented with 200 units/ml of penicillin, 40 μg/ml of streptomycin, and 10% fetal bovine serum. Cells were cultured at 37°C in a humidified and hypoxic atmosphere (5% O_2 and CO_2) to avoid acceleration of cell senescence as a result of oxidative stress (24,25).

RNA extraction and real-time polymerase chain reaction (PCR) analysis. Cells were seeded at a density of 1×10^5 cells/well in 24-well plates and allowed to grow to 70% confluence and then to 100% confluence. All experiments were performed in triplicate for each lot, and 2 different lots were used for this analysis. Cell pellets were resuspended in 350 μl of RNeasy (RLT) lysis buffer from an RNeasy kit and homogenized through QIAshredder columns (all from Qiagen Valencia, CA). RNA was extracted using RNeasy columns according to the manufacturer's instructions. Extracted RNA was eluted in 30 μl of RNase-free water. Single-strand complementary DNA (cDNA) was prepared from total RNA using a random primer under standard conditions and with a High-Capacity cDNA Reverse Transcription kit (Applied Biosystems, Foster City, CA). The cDNA from each sample was diluted and used to quantify the expression of type II collagen, aggrecan, and β-actin.

Quantitative real-time PCR with total cDNA was performed using Perfect Real-Time SYBR Green II (Takara Bio, Shiga, Japan) and the following primer sets: for β-actin, 5′-GGTCATCACCATTGGCAATG-3′ (forward) and 5′-CCACAGGACTCCATGCCC-3′ (reverse); for type II collagen, 5′-TGGTATCGCCGGACCCAAG-3′ (forward) and 5′-CTCGTCCACCGTCCTTCCC-3′ (reverse); and for aggrecan, 5′-CACCTGTAAAAAGGGCACAGTG-3′ (forward) and 5′-GCATTGATCTCGTATCGGTCC-3′ (reverse). The primer sets were designed to span exons in order to distinguish cDNA from genomic DNA products. PCR amplifications were performed using the 7700 real-time PCR system (Applied Biosystems) under the following conditions: 95°C for 10 seconds, followed by 40 cycles of 95°C for 5 seconds and 60°C for 30 seconds. To quantify the relative expression of each gene, the C_t values were normalized against the endogenous reference (ΔC_t = C_t target − C_t β-actin) and were compared with a calibrator, using the $\Delta\Delta C_t$ method ($\Delta\Delta C_t$ = ΔC_t sample − ΔC_t